

A FLIGHT TEST DETERMINATION OF THE
STATIC AND DYNAMIC LONGITUDINAL STABILITY
OF THE CESSNA 310H AIRCRAFT

William Harvey Siren

Library
Naval Postgraduate School
Monterey, California 94040

NAVAL POSTGRADUATE SCHOOL

Monterey, California



THESIS

A FLIGHT TEST DETERMINATION OF THE
STATIC AND DYNAMIC LONGITUDINAL STABILITY
OF THE CESSNA 310H AIRCRAFT

by

William Harvey Siren

June 1975

Thesis Advisor:

Donald M. Layton

Approved for public release; distribution unlimited.

SECURITY CLASSIFICATION OF THIS PAGE (When Data Entered)

DD FORM 1 JAN 73 1473
(Page 1)

Unclassified
SECURITY CLASSIFICATION OF THIS PAGE (When Data Entered)

The longitudinal long period, or phugoid, mode was investigated for the stick-fixed and stick-free cases and for widely separated center of gravity locations.

A Flight Test Determination of the
Static and Dynamic Longitudinal Stability
of the Cessna 310H Aircraft

by

William Harvey Siren
Lieutenant Commander, United States Naval Reserve
B.S., Stanford University, 1962
M.B.A., University of Miami, 1970

Submitted in partial fulfillment of the
requirements for the degree of

MASTER OF SCIENCE IN AERONAUTICAL ENGINEERING

from the

NAVAL POSTGRADUATE SCHOOL
June 1975

ABSTRACT

An investigation was made of the static and dynamic longitudinal stability of a Cessna 310H aircraft. Stick-fixed and stick-free neutral points were determined for both the cruise and approach configurations. Stick-fixed and stick-free maneuver points were determined for the cruise configuration. Values of the neutral points and maneuver points were also obtained from a theoretical analysis for comparison purposes. The longitudinal long period, or phugoid, mode was investigated for the stick-fixed and stick-free cases and for widely separated center of gravity locations.

TABLE OF CONTENTS

I.	INTRODUCTION-----	13
II.	EQUIPMENT-----	17
A.	TEST AIRPLANE-----	17
B.	INSTRUMENTATION-----	19
1.	General-----	19
2.	Power Supply-----	19
3.	Stick Force-----	20
4.	Elevator Angle-----	20
5.	Accelerometer-----	21
6.	Standard Aircraft Instruments-----	22
III.	PROCEDURE-----	24
A.	CENTER OF GRAVITY DETERMINATION-----	24
B.	PROCEDURE, GENERAL-----	25
C.	NEUTRAL POINTS-----	26
1.	Flight Tests-----	26
2.	Data Reduction-----	27
D.	MANEUVER POINTS-----	28
1.	Flight Tests-----	28
2.	Data Reduction-----	29
E.	PHUGOID-----	30
1.	Flight Tests-----	30
2.	Data Reduction-----	31
IV.	THEORETICAL ANALYSIS-----	32
A.	THEORETICAL DEVELOPMENT-----	32

B.	CALCULATIONS-----	35
1.	Reference Parameters-----	35
2.	Calculations-----	36
V.	DISCUSSION OF RESULTS-----	40
VI.	CONCLUSIONS AND RECOMMENDATIONS-----	43
A.	CONCLUSIONS-----	43
B.	RECOMMENDATIONS-----	44
	APPENDIX A: FIGURES-----	46
	LIST OF REFERENCES-----	75
	INITIAL DISTRIBUTION LIST-----	76

LIST OF FIGURES

1.	Cessna 310H Aircraft-----	46
2.	Cessna 310H Dimensions-----	47
3.	Instrument Console-----	48
4.	Instrumentation System-----	49
5.	Force Measuring Wheel-----	50
6.	Elevator Force Calibration-----	51
7.	Elevator Position Calibration-----	52
8.	Accelerometer Calibration-----	53
9.	δ_e vs. V_{cal} Cruise Configuration-----	54
10.	δ_e vs. C_L Cruise Configuration-----	55
11.	$\frac{\partial \delta_e}{\partial C_L}$ vs. % MAC Cruise Configuration-----	56
12.	F_S vs. V_{cal} Cruise Configuration-----	57
13.	F_S/q vs. C_L Cruise Configuration-----	58
14.	$\frac{d(F_S/q)}{dC_L}$ vs. % MAC-----	59
15.	N_O and N_O' vs. C_L Cruise Configuration-----	60
16.	δ_e vs. V_{cal} Approach Configuration-----	61
17.	δ_e vs. C_L Approach Configuration-----	62
18.	$\frac{\partial \delta_e}{\partial C_L}$ vs. % MAC Approach Configuration-----	63
19.	F_S vs. V_{cal} Approach Configuration-----	64
20.	F_S/q vs. C_L Approach Configuration-----	65
21.	$\frac{d(F_S/q)}{dC_L}$ vs. % MAC Approach Configuration-----	66
22.	N_O and N_O' vs. C_L Approach Configuration-----	67
23.	δ_e vs. n Cruise Configuration-----	68

24.	$\frac{\partial \delta_e}{\partial n}$ vs. % MAC Cruise Configuration-----	69
25.	F_s vs. n Cruise Configuration-----	70
26.	$\frac{dF_s}{dn}$ vs. % MAC-----	71
27.	N_m and N_m' vs. n Cruise Configuration-----	72
28.	Phugoid Characteristics Controls Free-----	73
29.	Phugoid Characteristics Controls Fixed-----	74

LIST OF SYMBOLS

a.c.	aerodynamic center
a_t	tail lift-curve slope
a_w	wing lift-curve slope
c	mean aerodynamic chord, (ft.)
c_e	elevator chord, (ft.)
c.g.	center of gravity
C_h	elevator hinge moment coefficient
C_{h_α}	$\partial C_h / \partial \alpha_t$
C_{h_δ}	$\partial C_h / \partial \delta_e$
C_L	lift coefficient
C_m	pitching moment coefficient
C_{m_δ}	elevator power coefficient
C_{n_p}	propeller normal force coefficient
$\frac{dC_m}{dC_L}$	stick fixed stability
D	propeller diameter, (ft.)
F_d	downspring force, (lb.)
F_s	stick force, (lb.)
G_e	elevator to stick gearing, (rad./ft.)
H	pressure altitude
l_e	distance from c.g. to center of pressure of tail, (ft.)
l_p	propeller moment arm, (ft.)
l_t	distance from wing a.c. to tail a.c., (ft.)

MAC	mean aerodynamic chord, (ft.)
n	normal load factor
N_m	stick-fixed maneuver point
N_m'	stick-free maneuver point
N_o	stick-fixed neutral point
N_o'	stick-free neutral point
P	period, (sec.)
q	dynamic pressure, (lb./sq. ft.)
S or S_w	wing area, (sq. ft.)
S_e	elevator area, (sq. ft.)
S_p	propeller disc area, (sq. ft.)
S_t	tail area, (sq. ft.)
T_c	thrust coefficient
V	velocity, (kt. or ft./sec.)
\bar{V}	tail volume coefficient
W	airplane gross weight, (lb.)
$X_{a.c.}$	distance of a.c. from leading edge of MAC, (ft.)
$X_{c.g.}$	distance of c.g. from leading edge of MAC, (ft.)
z	vertical location of thrust line from c.g., (ft.)

GREEK SYMBOLS

α	angle of attack, (deg. or rad.)
δ	control deflection, (deg.)
$(\frac{d\beta}{d\alpha})_{prop}$	wing upwash derivative evaluated at the propeller
$d\epsilon/d\alpha$	wing downwash derivative
$d\epsilon_p/d\alpha$	propeller downwash derivative
η_p	propeller efficiency

η_t	tail efficiency, q_t/q
ρ	air density, (slugs/cu. ft.)
τ	elevator effectiveness
ζ	damping ratio

SUBSCRIPTS

a.c.	aerodynamic center
c.g.	center of gravity
e	elevator
p	propeller or phugoid
s	stick or slipstream
t	tail
w	wing

ACKNOWLEDGEMENT

The author is indebted to several people for their assistance in the completion of this investigation. A special debt of gratitude is owed to Associate Professor Donald M. Layton whose ideas and guidance provided the foundation for this project. His inspiration, humor, and technical knowledge made the investigation both stimulating and educationally rewarding.

Administrative assistance was received from Commander J. B. Poland who also patiently served as instructor pilot in qualifying the author as a command pilot in the research aircraft.

The fabrication and installation of the test equipment were done by Aeronautics Department technical personnel under the direction of Mr. Robert Besel and Mr. Theodore Dunton. The author is especially grateful to Mr. Cecil Gordon, who designed much of the instrumentation system, and to Mr. Bertis Funk, who provided invaluable assistance in installing and calibrating the system.

The author also wishes to acknowledge with gratitude the opportunity for postgraduate education provided by the United States Navy.

I. INTRODUCTION

The purpose of this investigation was to determine the variation of the aircraft neutral points (N_o and N_o') with lift coefficients, the variation of the maneuver points (N_m and N_m') with normal acceleration, and the aircraft's dynamic response to a sudden longitudinal control force input. The test aircraft was a Cessna model 310H used in the flight evaluation techniques courses, Department of Aeronautics, Naval Postgraduate School.

The stick-fixed (control position) and stick-free (control force) static stability of an airplane can be determined from steady state flight tests by measuring the deflection of the longitudinal control surface and the stick or wheel force at various airspeeds and normal accelerations. Analysis of such data typically indicates the nature of the stability levels of the aircraft in the form of variations of the neutral point with lift coefficient and the maneuver point with normal acceleration. The neutral point is that center of gravity location where the pitching moment is independent of angle of attack; i.e., where the static stability is neutral. The maneuver point is that center of gravity location where the gradient of the elevator angle per g (or stick force per g in the stick free case) reverses sign.

Dynamic longitudinal stability of an aircraft is generally determined by analyzing its long period ("phugoid") and short

period characteristics. Airspeed (or altitude) variation with time following an elevator control input provides the information necessary to determine the dynamic characteristics (period and damping ratio) of the aircraft.

Several methods have been utilized for obtaining static longitudinal stability data in flight. In determining the location of the neutral points, flight test methods include the "slow acceleration-deceleration technique," the "power acceleration-deceleration technique," the "effective weight moment" method, the "tab angle" method, and the "stabilized point" technique (or the "elevator angle and stick force vs. airspeed" method).

The elevator angle and stick force vs. airspeed method was used in this investigation. This technique obviates the need for automatic recording devices and reduces the time for data reduction, which are drawbacks of some of the other alternatives. References 1, 2, and 3 offer excellent descriptions of these various flight test methods for determining static longitudinal stability.

In the determination of airplane maneuver points, there are three basic test techniques that are used to obtain elevator angle and stick force vs. normal acceleration data. These are the "steady pull-up" method (or its reverse, the "steady pushover" method), the "wind-up turn" method (or its reverse, the "wind-down turn" method), and the "steady-turn" technique. These methods are well described in Ref. 3.

The steady-turn technique was chosen for this project. This method involves obtaining data at a constant longitudinal trim setting, a constant power setting, and a constant airspeed (trim airspeed) while varying normal acceleration by varying pitch rate during stabilized turns. This method is somewhat simpler than the steady pull-up technique because the test pilot has a better opportunity to stabilize exactly on trim airspeed and normal acceleration. The altitude loss is also less in this maneuver than in either of the two alternative maneuvers. Additionally, because of the nature of the technique, the stabilized condition can be maintained for a longer time period which facilitates obtaining the necessary data. Finally, the instrumentation requirements are less severe than in the wind-up turns, and less flight time is required than in the steady pull-ups.

The flight test technique in determining the phugoid characteristics simply involved stabilizing the aircraft at an airspeed 15 knots faster than trim airspeed, returning the controls to the trim position, and then recording a time history of the airspeed variation. This technique is also described in Ref. 1. Short period characteristics were not quantitatively determined since that investigation would have required even more special instrumentation.

For purposes of comparison with flight results, theoretical values of the neutral points and maneuver points were determined for the cruise configuration at an appropriate lift coefficient. This theoretical analysis is included in Section IV of this report.

All flight tests for this investigation were conducted at Monterey, California during the second quarter of fiscal year 1975.

II. EQUIPMENT

A. TEST AIRPLANE

The aircraft used for the flight test program was a Cessna 310H, registration number N164X. It is a six-place, low-wing, twin-engine monoplane with fully retractable landing gear, and it is powered by two horizontally opposed, six-cylinder, Continental Model IO-470-D engines rated at 260 horsepower at 2625 RPM. The aircraft is equipped with all-metal, hydraulically operated, constant speed, full-feathering, two-bladed propellers. Conventional wheel and rudder pedal controls operate the primary control surfaces, each of which has an adjustable trim tab, and the elevator is fitted with a downspring.

Although the Cessna 310H is basically a six-place aircraft, the Naval Postgraduate School's 310H has been configured with four seats. The rear seats have been removed to provide space for part of the special instrumentation system used in the Department of Aeronautics' courses in Flight Evaluation Techniques. A photograph and three-view drawing of the aircraft are shown in Figs. 1 and 2.

1. Airplane, General

Length (overall)	29.50 ft.
Height	9.94 ft.
Design gross weight	5,100 lb.

2. Wing

Area (total)	175 sq. ft.
Span	36.92 ft.

Type	Full cantilever
Airfoil (centerline)	NACA 23018
Airfoil (tip)	NACA 23009
Airfoil (nacelle)	NACA 23012
Incidence (root)	+2° 30'
Incidence (tip)	-0° 30'
Mean aerodynamic chord	61 in.
Taper ratio	1.517
Aspect ratio	7.0
Dihedral	5°
Area (flap)	22.9 sq. ft.
Angular travel (flap down)	45° +1° -0°
Leading edge of MAC from Datum plane	22.25 in.

3. Horizontal Tail

Span (total)	17 ft.
Airfoil (root)	NACA 0009
Airfoil (tip)	NACA 0006
Incidence	-1° 45'
Area (total)	54.25 sq. ft.
Area (stabilizer)	32.15 sq. ft.
Area (elevator)	22.10 sq. ft.
Tail a.c. from wing a.c.	175 in.
Elevator to stick gearing ratio	0.98 rad./ft.
Elevator chord (average)	1.3 ft.

B. INSTRUMENTATION

1. General

Aside from the aircraft's standard instruments, the only instrumentation devices required for neutral point and maneuver point determination were for the measurement of stick force, elevator angle, and normal acceleration. A small portable console, containing instrumentation for reading elevator angle, stick force, and normal acceleration in the form of voltage (which was subsequently converted to a value for the desired parameter) was designed in previous research work and was used in this investigation. The portable feature of the console enabled it to be positioned securely between the pilots or facing aft at the top rear of the copilot's seat. Because of this arrangement, crew requirements were flexible. The instrument console is shown in Fig. 3, and a block diagram of the instrumentation system is shown in Fig. 4. The instrumentation system consisted of a junction box (J-box) which collected inputs from the stick force, elevator position, and normal acceleration electrical sensors, wire plug-in jacks for patching signals to the instrument console, a five-position two-pole rotary switch in the console, and a Datel DM-1000 digital voltmeter in the console.

2. Power Supply

The aircraft electrical system, consisting of two 25-ampere engine-driven generators and two 12-volt batteries, provided 24-volt direct current power to the instrumentation system.

3. Stick Force

The standard copilot's control wheel was replaced by a special wheel built for stick force measurement. Figure 5 shows the force measuring wheel installed in the aircraft. Four C-9-171 strain gages were installed on the cross beam of the wheel and were wired to form a 350-ohm wheatsone bridge circuit. The bridge output was connected to a Grant model DCA8-3 differential amplifier, in order to increase the strain gage bridge output and decrease the noise level. The differential amplifier then supplied the J-box with the appropriate electrical signal. To calibrate the stick force, a known force was applied in both directions at the vertical handgrips on the control wheel and the gain and zero settings were adjusted on the amplifier to provide a proper response to the known force. The elevator force response was linear for the force applications encountered in the investigation. The elevator force calibration curve is shown in Fig. 6.

4. Elevator Angle

Since the control surfaces of the Cessna 310H are positioned by purely mechanical linkages of cables, pulleys, and bell-cranks, determination of the elevator position was accomplished by measuring the displacement of the elevator linkage assembly. A linear displacement transducer, which consisted of a 2,000-ohm rotating-arm potentiometer enclosed in an aluminum housing, was mounted in the rear fuselage section of the aircraft. A flexible wire cable, wound around a spring-loaded drum in the potentiometer, was fastened to the

elevator bell-crank. Elevator deflection, then, was sensed by a change in slide contact resistance inside the potentiometer. A 5,000-ohm balance potentiometer was mounted in parallel with the linear displacement transducer forming a bridge circuit to allow voltage nulling for zero control deflection. To avoid exceeding the voltmeter limitation and to provide the necessary regulated voltage for the bridge, the aircraft 24-volt electrical supply was reduced to 5 volts through the use of a National Semiconductor voltage regulator. The voltage regulator was mounted within the J-box near the position circuit balance potentiometer.

To calibrate the elevator position, the elevator was first locked into a zero deflection position with "C" clamps. The balance potentiometer was adjusted for a zero voltage reading. Then, using an Angle Finder (a precision protractor), the elevator was deflected in small increments to its extremes of travel and voltage readings were taken for each position. The elevator position calibration curve is shown in Fig. 7.

5. Accelerometer

A Statham model ASTC-8.0-350 accelerometer was used to measure the aircraft's normal acceleration. Construction in this model is of the unbonded strain gage design which has the strain gages attached to a fixed frame and to a force summing member. When the force summing member is displaced, the balance of the bridge is changed, providing an electrical output proportional to the magnitude of the applied force. A Grant differential amplifier was used with the accelerometer

to give an output of 100 millivolts per g. The accelerometer was mounted on the aircraft's deck, slightly aft of the rear seats. The output of the differential amplifier went to the J-box.

This accelerometer was statically calibrated on a centrifuge for a previous project and found to have a linear output in the range of -2 to +6 g's. As a result, the only calibration required was the two-g turnover method to adjust the zero and gain of the amplifier for the desired output. The transducer was first placed on a level platform with its sensitive axis perpendicular to the earth's gravitational field. The output of the Grant differential amplifier was then zeroed for this zero-g condition. The accelerometer was then rotated to the positive one-g condition and the amplifier output was adjusted to +100 millivolts. It was then rotated to the negative one-g condition and the amplifier was adjusted to -100 millivolts. A standard mechanical accelerometer was also installed in the aircraft for gross in-flight checks of the Statham accelerometer. The accelerometer calibration curve is shown in Fig. 8.

6. Standard Aircraft Instruments

Airspeed, altitude, fuel quantity, and outside air temperature were determined by using the airplane's standard instruments. Airspeed calibration data were taken from a manual published by the manufacturer. The outside air temperature gage was determined to be quite accurate on the ground when compared to a precision thermometer. The fuel tank quantity

gages were not calibrated, but it was determined that errors in quantity readings would be small and would have negligible effects on center of gravity determination. No attempt was made to calibrate the altimeter since it was used for general reference only.

III. PROCEDURE

A. CENTER OF GRAVITY DETERMINATION

The aircraft was weighed by using four Baldwin-Lima-Hamilton SR-4 load cells. The load cells were secured between each of four jacks and the aircraft's jack points. The load cells, rated at 5,000 lbs. each, utilize bonded strain gages, and were laboratory calibrated with a Riehle 300,000 lb. compression testing machine. The aircraft was weighed in both the gear up and gear down configurations in order to determine the basic weight and c.g. locations. The moment of the airplane was calculated with respect to Station 0.0, hereafter known as the Datum. By knowing the weights at each of the jack points and by measuring the associated moment arms, the center of gravity of the aircraft was obtained. The weight and moment arm of the basic aircraft were obtained by correcting the gross data for the fuel and oil that were aboard when the aircraft was weighed. The moment arms for each of the seat locations and for the ballast location were accurately measured. The moment arms for the fuel and oil tanks were not measured; the values provided by the manufacturer were used in all computations in this report. Special care was taken to ensure that no fuel was consumed out of the auxiliary fuel tanks. Hence, center of gravity determination for each flight test required no adjustment for auxiliary tank fuel consumed in flight.

Having the values for the basic airplane moment, basic airplane weight, weights of the pilots, passengers, and/or ballast, and also knowing the moment arm for fuel and each location in the cabin, the weight and moment (hence, c.g. location) was determinable for the airplane under any loading condition.

Weight and balance information is summarized in tabular form below.

	<u>Weight</u>	<u>Moment about Datum</u>
Basic airplane, gear up (includes oil and full aux. fuel tanks)	3,605 lb.	133,496 in.-lb.
Basic airplane, gear down	3,605 lb.	132,100 in.-lb.
Moment arms from Datum for variable loads:		
Main fuel	35 in.	
Pilots	38 in.	
Aft passenger seats	71 in.	
Ballast	126 in.	

B. PROCEDURE, GENERAL

In general, the procedures used in this investigation for both flight testing and data reduction follow the guidelines set forth in Ref. 3. Although only two center of gravity locations are theoretically needed, three or four widely spaced locations were used in each test in order to account for any possible nonlinearities and to reduce experimental error. The variation in c.g. location was obtained by varying the number of people on the aircraft and/or by carrying ballast. A total shift in c.g. location of about seven per cent mean aerodynamic chord (MAC) was thus obtained for each configuration.

Two airplane configurations were investigated: the cruise configuration (CR), and the landing approach configuration (LA). Maneuvering tests were performed only in the cruise configuration since maneuvering stability in the approach configuration is normally of little interest.

The cruise configuration, as used herein, was with landing gear and flaps retracted and a trim speed of 150 knots. The cruise power setting used was that required for level flight at the trim airspeed and at a pressure altitude of 6,000 feet.

In the approach configuration, the landing gear were down and the flaps were set at 30° . The trim speed was 100 knots. The approach power setting was again that required for level flight at the trim airspeed and at an altitude of 6,000 feet. It is normally desirable that the approach configuration tests be conducted at a relatively low altitude. However, it was necessary to fly at an average test altitude of 6,000 feet to avoid low stratus clouds or the low altitude turbulence that creates annoying yawing oscillations in the Cessna 310H.

C. NEUTRAL POINTS

1. Flight Tests

As previously mentioned, the neutral points were found for both the cruise configuration and the power approach configuration. The same flight test procedure was used for each condition. First, the approximate c.g. position was selected and the passenger and ballast requirements were determined accordingly. Flights for various c.g. positions were all conducted on different days because of the nature of the method chosen to change the c.g. location.

The inflight procedure involved trimming the aircraft at the trim speed and at the test altitude. Once power and trim settings were made for a given configuration, neither was changed for the test at that c.g. location. The airspeed was then changed and stabilized by applying an elevator input. When steady state conditions were reached, the elevator position and stick force indicator readings were recorded. Airspeeds were alternately increased and decreased from the trim speed in an effort to maintain a constant altitude. Approximately a 50-knot range was covered in 5-knot increments. Taking about ten steady state airspeeds tended to reduce experimental error and nonlinearities. Special care (and rudder action) was taken by the pilot to ensure that zero sideslip was maintained for all test airspeeds.

2. Data Reduction

All of the recorded data were corrected or put into the proper form by referring to the appropriate calibration curves, and the c.g. location was computed as a percentage of the mean aerodynamic chord for each c.g. position. The subsequent analysis follows the same procedure for both configurations.

Elevator positions and stick force were plotted against calibrated airspeed for each c.g. location as a first step in the analysis. These plots produced curves that were smoothed through points which were relatively evenly spaced throughout the speed range tested. Then the curves of elevator angle vs. lift coefficient and stick force divided by dynamic pressure

vs. lift coefficient were drawn. See, for example, Figs. 10 and 13. Slopes of these curves were then taken at various values of lift coefficient and plots were made of $\frac{\partial \delta_e}{\partial C_L}$ vs. % MAC and of $\frac{dF_s/q}{dC_L}$ vs. % MAC for the various values of lift coefficient. See Figs. 11 and 14. By definition, the neutral points, N_0 and N_0' are the c.g. locations at which $\frac{\partial \delta_e}{\partial C_L}$ and $\frac{dF_s/q}{dC_L}$, respectively, are zero. Hence, the neutral points were then determinable for the various lift coefficients by extrapolation. See Fig. 15 for a summary of the neutral points for the cruise configuration and Fig. 22 for the neutral points for the approach configuration.

D. MANEUVER POINTS

1. Flight Tests

The maneuver points were determined by an analysis of elevator angle and stick force data taken at various values of normal acceleration -- all at the same airspeed. Occasionally there are small differences in data obtained in left hand and right hand turns due to gyroscopic effects when using the steady-turn maneuver. Preliminary testing showed this difference to be minor in the Cessna 310H, and all data for this investigation were taken in left hand turns.

The maneuver points were found for the same cruise configuration as used in the neutral point flight tests, i.e., the same trim airspeed, test altitude, and approximately the same power setting. There was, of course, an altitude loss in this maneuver due to the reduction in the vertical component of the lift vector. Errors due to altitude loss were minimized,

however, by returning to the test altitude prior to each turn. The c.g. conditions were selected as described for the neutral point flight tests and the airplane was trimmed for hands-off flight. The power and trim settings remained unaltered throughout the test at any one c.g. condition. The airplane was placed in a left hand turn and when steady flight conditions were established (constant airspeed at V_{trim} , zero sideslip, and a constant angle of bank), the normal acceleration, elevator position, and the stick force indications were recorded. The normal acceleration was rechecked, and the bank angle was held until all three readings had stabilized. This process was repeated for several bank angles between 0° and 60° .

2. Data Reduction

As in the neutral point analysis, the recorded data were corrected and put into the proper form by referring to the appropriate calibration curves and the c.g. location was computed as a percentage of MAC for each of the c.g. conditions tested.

The elevator angle and the stick force were each plotted against the normal force factor, n (see Figs. 23 and 25). The slope of these curves was then taken at various values of normal acceleration and plotted against percentage of MAC (Figs. 24 and 26) resulting in the maneuver points as the intersections on the abscissa of each graph. See Fig. 27 for a summary plot showing the variation of N_m and N_m' with n .

E. PHUGOID

1. Flight Tests

The phugoid characteristics were determined by analysis of the time history of the airspeed variation when the aircraft was longitudinally disturbed from its trim position.

The c.g. positions were selected as described earlier, but since the primary purpose here was to determine the effect of c.g. position on the phugoid characteristics, only two widely spaced c.g. positions were needed.

The phugoid characteristics were determined for both the controls-free and controls-fixed cases. In the former, the aircraft was trimmed for level flight at 140 knots, 6000 ft., and at an appropriate power setting. A mark was then placed on the control column where it enters the column sleeve. Then, using elevator control alone, the aircraft's speed was stabilized at 155 knots. Controls were then returned to the original trim position and released to initiate the controls-free oscillation. A stopwatch was started as the aircraft's speed first passed through 140 knots. Airspeed and elapsed time were recorded as the aircraft passed through its maxima, minima, and trim speeds. Slight rudder inputs were occasionally needed to prevent any rolling tendencies.

The procedure for the controls-fixed case was exactly the same as that described above with the exception that when the controls were returned to the trim position, the control column was manually and rigidly restrained in that position. The airspeed-time history was again recorded and the effect

of elevator "float" could then be seen as the difference between the phugoid characteristics performed with controls free and controls fixed.

2. Data Reduction

Center of gravity locations were computed in the standard manner and plots were made for airspeed vs. time for the two c.g. locations for both the controls-fixed and controls-free cases. The period for each phugoid motion was determined by subtracting the time for the first maximum airspeed from that for the last maximum airspeed and dividing that time by the number of included cycles. The damping ratio, ζ_ρ , was calculated from the formula:

$$\ln \left(\frac{A_1}{A_2} \right) = \frac{2\pi\zeta}{\sqrt{1 - \zeta^2}}$$

where A_1 and A_2 are consecutive maximum excursions from the final stabilized airspeed. The damping ratio was computed for each cycle and then averaged for the number of measurable cycles. See Figs. 28 and 29 for a summary of the phugoid characteristics.

IV. THEORETICAL ANALYSIS

A. THEORETICAL DEVELOPMENT

The theoretical determination of the various stability derivatives and other pertinent parameters was based primarily on methods given in Ref. 4 and data provided in Ref. 5. The neutral points and maneuver points were theoretically estimated for the cruise configuration using actual conditions encountered in the flight tests.

For steady state flight, the equation for the summation of moments about the airplane center of gravity can be written:

$$C_{m_{cg}} = C_{L_w} \frac{X_a}{c} + C_{mac} + C_{m_{FUS,NAC}} - C_{L_t} \bar{V} \eta_t + 4 \frac{T_c}{S_w} D^2 \frac{z}{c} \\ + 2 C_{n_p} \frac{l_p}{c} \frac{S_p}{S_w} = 0$$

where the last two terms represent the influence of running propellers.

For this analysis, the center of gravity of the aircraft and the aerodynamic center of the wing were assumed to be co-located. Therefore,

$$\frac{X_a}{c} = 0$$

The stability derivative $\frac{dC_m}{dC_L}$ can now be found by taking the derivative of the moment equation with respect to C_L .

$$\frac{dC_m}{dC_L} = \frac{dC_m}{dC_{L_{FUS,NAC}}} - C_{L_t} \bar{V} \frac{d\eta_t}{dC_L} - \frac{a_t}{a_w} \bar{V} \eta_t \left(1 - \frac{d\epsilon}{d\alpha} - \frac{d\epsilon_p}{d\alpha}\right) \\ + \frac{dT_c}{dC_L} \frac{4D^2 z}{S_w c} + \frac{dC_{n_p}}{dC_L} \frac{l_p}{c} \frac{S_p}{S_w}$$

The determination of the various derivatives is shown in the "Calculations" subdivision of this section, and values of the various required airplane dimensions are shown in the table of airplane specifications. The tail lift coefficient, C_{L_t} , was found by solving the moment equation for the tail force required to trim the airplane.

The control-fixed neutral point, N_0 , can now be determined, since

$$N_0 = X_{cg} - \frac{dC_m}{dC_L}$$

In computing the control-free neutral point, N_0' , it is necessary to consider the effect of the stick force due to the downspring in the elevator control system. This force, F_d , was measured for various elevator positions and the value for the test condition to be compared to the theoretical results is included in subsequent calculations. The control-free neutral point can now be estimated from:

$$N_0' = N_0 + \frac{C_{m_\delta} C_{h_\alpha}}{a_w C_{h_\delta}} \left(1 - \frac{d\epsilon}{d\alpha}\right) + \frac{F_d C_{m_\delta}}{G_e S_e c_e C_{h_\delta} W/S}$$

The elevator power, C_{m_δ} , can be computed from:

$$C_{m_\delta} = -a_t \bar{V} \eta_t \tau$$

Values of C_{h_α} and C_{h_δ} were obtained from wind tunnel data for the Cessna 310H as provided by Ref. 5. The elevator gearing ratio, G_e , was measured on the control system of the airplane and is listed in the airplane specifications.

The maneuvering points can now be calculated. For steady turning flight:

$$N_m = N_o - \frac{63gl_t \rho C_{m\delta}}{2(W/S)\tau} (1 + \frac{1}{n^2})$$

And,

$$N_m' = N_o' + \frac{57.3 C_{m\delta}}{(W/S)C_{h\delta}} [\frac{\rho}{2} g l_t (C_{h\alpha} - \frac{1.1 C_{h\delta}}{\tau})] (1 + \frac{1}{n^2})$$

where n is the normal acceleration.

The contribution of the downspring to N_o' must be neglected in the above equation since it has no effect on the control-free maneuvering point.

The significant results of this analysis have been extracted from the "Calculations" subdivision of this section and are shown below. The results are for flight test conditions where the center of gravity was close to the wing aerodynamic center. These flight test conditions are also listed below. A value of $n = 1.6$ was arbitrarily selected for maneuvering point calculations.

<u>Parameter</u>	<u>Theoretical Value</u>
N_o	0.499
N_o'	0.649
N_m	0.597
N_m'	0.532

Test Conditions

$V = 150$ kts.

$h = 6,000$ ft. pressure altitude

$W = 4,506$ lb.

c.g. = 24.02 % MAC

B. CALCULATIONS

1. Reference Parameters

In addition to the information presented in the table of airplane specifications, the following data was used in the theoretical calculations:

$a_w = 0.0813$	(Ref. 4)
$\tau = 0.59$	(Ref. 4)
$\rho = 0.001988$	(Ref. 4)
$C_{m_{a.c.}} = -0.01$	(Refs. 4 & 5)
$\frac{d\varepsilon}{d\alpha} = 0.375$	(Ref. 5)
$\left(\frac{dC_n}{d\alpha}\right)_p \text{ TC}=0 = 0.00165$	(Ref. 4)
$\frac{d\varepsilon_p}{d\alpha} = 0.0504$	(Ref. 4)
$\left(\frac{d\beta}{d\alpha}\right)_{\text{prop}} = 1.25$	(Ref. 4)
$X_{a.c.} = 0.245$	(Ref. 6)
$C_{h_\alpha} = -0.1146$	(Ref. 5)
$C_{h_\delta} = -0.5909$	(Ref. 5)
$C_{m_\delta} = -0.0365$	(Ref. 5)
$\eta_p = 0.85$	(Ref. 4)
$W = 4506 \text{ lb.}$	Flight test
$V = 150 \text{ kts.} = 253.2 \text{ ft./sec.}$	Flight test
$H = 6000 \text{ ft.}$	Flight test
$C_L = 0.344$	Flight test
$c.g. = 24.02 \% \text{ MAC}$	Flight test

2. Calculations

a. Tail Efficiency, η_t

$$T_c = \frac{\text{BHP } \eta_p^{550} C_L^{3/2} \rho^{1/2}}{(2W/S)^{3/2} D^2} \quad (\text{Ref. 4})$$

$$T_c = \frac{(138)(.85)(550)(.344)^{3/2}(.001988)^{1/2}}{[2(4506)/(175)]^{3/2}(6.67)^2} = 0.0353$$

$$\eta_t = \frac{V_s}{V} = \left(\frac{1+8T_c}{\pi} \right) \quad (\text{Ref. 7})$$

$$\eta_t = 1 + 2.55 (.0353) = 1.09$$

b. Tail Volume, \bar{V}

$$\bar{V} = \frac{l_t S_t}{S c} \quad (\text{Ref. 6})$$

$$\bar{V} = \frac{14.59(54.25)}{175(5.083)} = 0.891$$

c. Tail lift-curve slope, a_t

$$a_t = \frac{-C_{m\delta}}{\bar{V}\eta_t\tau} \quad (\text{Ref. 4})$$

$$a_t = \frac{-(-.0365)}{(.891)(1.09)(.60)} = 0.0626$$

d. Fuselage and nacelle contribution to $\frac{dC_m}{dC_L}$:

$$\left(\frac{dC_m}{dC_L} \right)_{\text{FUS}, \text{NAC}} = \frac{K_f w_f^2 L_f}{S_w c a_w} + \frac{K_n w_n^2 L_n}{S_w c a_w} \quad (\text{Ref. 4})$$

where L_f and L_n are fuselage and nacelle lengths, w_f and w_n are maximum widths of the fuselage and nacelle, and K_f and K_n are empirical factors given in Ref. 4.

$$\begin{aligned} \left(\frac{dC_m}{dC_L} \right)_{\text{FUS, NAC}} &= \frac{(.008)(4.353)^2(26.45)}{175(5.083)(.0813)} \\ &+ \frac{2(.04)(3.11)^2(8.81)}{175(5.083)(.0813)} = 0.160 \end{aligned}$$

e. Estimation of Propeller Effects:

$$\frac{dT_c}{dC_L} = (3/2) K \eta_p C_L^{1/2} \quad (\text{Ref. 4})$$

where

$$K = \frac{\text{BHP}(550) \rho^{1/2}}{(2W/S)^{1.5} D^2} = \frac{(138)(550)(.001988)^{1/2}}{[2(4506)/(175)]^{1.5} (6.67)^2} = 0.206$$

$$\frac{dT_c}{dC_L} = 1.5(.206)(.85)(.344)^{1/2} = 0.154$$

$$\frac{z}{c} = 0.066 \quad (\text{estimated from three-view drawing})$$

$$\frac{dC_{np}}{dC_L} = \frac{dC_{np}}{d\alpha_p} \frac{d\alpha_p}{dC_L} = \frac{dC_{np}}{d\alpha_p} \frac{(1 + \frac{d\epsilon}{d\alpha})}{a_w} \quad (\text{Ref. 4})$$

$$\frac{dC_{np}}{d\alpha_p} = 0.146 \quad (T_c = .0353) \quad (\text{Ref. 8})$$

$$\frac{dC_{np}}{dC_L} = \frac{(.146)(1 + .375)}{(.0813)(57.3)} = 0.0434$$

$$\frac{d\eta_t}{dC_L} = \frac{d\left(\frac{V_s}{V}\right)^2}{dC_L} = \frac{8}{\pi} \frac{dT_c}{dC_L} = 2.54(.154) = 0.392$$

f. Tail Lift Coefficient, C_{Lt} :

Assuming constant derivatives,

$$C_{m_{c.g.}} = 0 = C_{m_{a.c.}} + C_L \left[\left(\frac{dC_m}{dC_L} \right)_{FUS, NAC} + \frac{dC_{np}}{dC_L} \frac{1_p}{c} \frac{s_p}{s_w} \right. \\ \left. + \frac{dT_c}{dC_L} \frac{4D^2}{S_w} \frac{z}{c} \right] - C_{L_t} \bar{V}_{\eta_t}$$

$$C_{L_t} = \frac{1}{(.891)(1.09)} \{ -.01 + .344 [.16 + (.0434) \left(\frac{5.15}{5.08} \right) \left(\frac{69.81}{175} \right) \\ + \frac{.154(4)(6.67)^2(.066)}{175}] \} = 0.053$$

g. Static Margin:

$$\frac{dC_m}{dC_L} = \left(\frac{dC_m}{dC_L} \right)_{FUS, NAC} - C_{L_t} \frac{\bar{V}_{d\eta_t}}{dC_L} - \frac{a_t}{a_w} \bar{V}_{\eta_t} \left(\frac{1-d\epsilon}{d\alpha} - \frac{d\epsilon_p}{d\alpha} \right) \\ + \frac{dT_c}{dC_L} \frac{4D^2}{S_w} \frac{z}{c} + \frac{dC_{np}}{dC_L} \frac{1_p}{c} \frac{s_p}{s_w}$$

$$\frac{dC_m}{dC_L} = .160 - .053(.891)(.392) - \frac{.0626}{.0813}(.891)(1.09)(1 - .375 - .0504) \\ + .154(4) \left(\frac{6.67}{175} \right)^2 (.066) + .0434(1.0137)(.399) = -0.259$$

h. Control-Fixed Neutral Point, N_O :

$$N_O = X_{c.g.} - \frac{dC_m}{dC_L}$$

$$N_O = .2402 - (-.259) = 0.499$$

i. Control-Free Neutral Point, N_O' :

$$N_O' = N_O + \frac{C_{m_\delta} C_{h_\alpha}}{a_w C_{h_\delta}} \left(1 - \frac{d\epsilon}{d\alpha} \right) + \frac{F_d C_{m_\delta}}{G_e S_e C_e C_{h_\delta} (W/S)}$$

$$N_O' = .499 + \frac{(-.0365)(-.1146)(1 - .375)}{(.0813)(-.5909)} \\ + \frac{42(-.0365)(57.3)}{.98(22.1)(1.3)(-.5909)\left(\frac{4506}{175}\right)}$$

$$N_O' = 0.649$$

j. Control-Fixed Maneuver Point, N_m :

$$N_m = N_O - \frac{63g \rho C_{m\delta} \left(1 + \frac{1}{n^2}\right)}{2(W/S) \tau}$$

$$N_m = .499 - \frac{63(32.2)(14.6)(.001988)(-.0365)\left[1 + \frac{1}{(1.6)^2}\right]}{2(4506/175)(.59)}$$

$$N_m = 0.597$$

k. Control-Free Maneuver Point, N_m' :

$$N_m' = N_O' + \frac{57.3C_{m\delta}}{(W/S)C_{h\delta}} \left[\frac{\rho}{2} g l_t (C_{h\alpha} - 1.1 \frac{C_{h\delta}}{\tau}) \right] \left(1 + \frac{1}{n^2}\right)$$

where the downspring effect is neglected in N_O' .

$$N_m' = .444 + \frac{57.3(-.0365)}{(4506/175)(-.5909)} \\ \left\{ \frac{.001988}{2} (32.2)(14.6) \left[-.1146 - 1.1 \frac{(.5909)}{.59} \right] \right\} \\ \left[1 + \frac{1}{(1.6)^2} \right]$$

$$N_m' = 0.532.$$

V. DISCUSSION OF RESULTS

The main results of this investigation are summarized in Figs. 15, 22, 27, 28, and 29. For the static stability study, a comparison of theoretical values and flight test results are listed below in tabular form. These results are for the cruise configuration only and for the flight conditions listed in Section IV.

<u>Parameter</u>	<u>Fraction of MAC</u>	
	<u>Theoretical</u>	<u>Flight Test</u>
N_0	0.499	0.446
N_0'	0.649	0.590
N_m	0.597	0.554
N_m'	0.532	0.452

Reasonably good agreement exists between the theoretical and flight test values. It can be seen from the theoretical analysis in Section IV that any error in the value of N_0 is carried through in the calculation of the other three parameters. The factors most influencing N_0 are wing and tail lift-curve slopes and tail efficiency; the difference in the theoretical and flight test values can probably be attributed to the difficulties in accurately estimating those factors.

The most apparent result shown in Figs. 15 and 22 is that the aircraft is much more stable "stick-free" than "stick-fixed." This result is due to the action of the strong downsprings in the elevator system and to the elevator's

horn balance. Figures 15 and 22 also show that stability decreases with increasing angle of attack -- a typical phenomenon in low-wing monoplanes.

Figures 15 and 27 indicate that N_m is aft of N_0 by about 10% of the mean aerodynamic chord. This result is typical for airplanes with tails, as indicated by Etkin in Ref. 6.

The maneuver points show a normal trend in that N_m' is forward of N_m . It can also be seen that the largest difference between the theoretical value and the flight test value for the four parameters investigated lies in N_m' . This indicates the difficulty in estimating the elevator hinge-moment derivatives and may indicate some error in the stick force measurements in the flight tests.

The dynamic stability investigation, represented in Figs. 28 and 29, shows a well-damped convergence for the phugoid mode. These figures also show that the period is shorter and the damping ratio is higher for the control-fixed case for a given center of gravity position. As mentioned earlier, the effect of elevator float can be seen as the difference between the phugoids performed with controls free and controls fixed. The fact that the aircraft did not always return to equilibrium flight at the original trim speed is attributable to a fairly large trim speed band.

For both the control-fixed and control-free phugoid observations, the frequency of the mode decreased (period became longer) and the damping remained essentially constant as the center of gravity was moved aft. (The damping ratio calculations

were based on airspeed observations which could be read no closer than one knot.) This effect of aft center of gravity movement on the phugoid mode is a typical response, and the theoretical justification for such a response is well described by Etkin in Ref. 6.

VI. CONCLUSIONS AND RECOMMENDATIONS

A. CONCLUSIONS

It is concluded that:

1. The instrumentation system installed in the Department of Aeronautics' Cessna 310H for flight evaluation purposes is reliable and capable of supplying sufficiently accurate flight test data.

2. Reasonably good correlation exists between theoretical and flight test data for the static stability investigation.

3. Static longitudinal stability, as indicated by the variation of longitudinal control force and elevator position about the trim airspeed, was positive in both configurations tested.

4. The Cessna 310H airplane has an unusually high degree of control-free stability due primarily to the effect of the strong downsprung.

5. There is a decrease in the static stability of the aircraft in the approach configuration.

6. The relative position of the maneuvering points of the Cessna 310H is normal in that N_m' is forward of N_m .

7. Stick-fixed stability is normal in that N_o is forward of N_m .

8. Dynamic longitudinal stability, as evidenced by the characteristics of the long period or phugoid mode, is positive for the normal range of center of gravity travel.

9. The short period longitudinal mode of the Cessna 310H is essentially deadbeat, indicating a good damping ratio and a medium to high short period undamped natural frequency.

B. RECOMMENDATIONS

It is recommended that:

1. An investigation be made into the power and attitude effects on the elevator hinge moment derivatives. It is further recommended that a study be made of the effects of wing and nacelle wake on the flow over the tail.

2. Static and dynamic stability be investigated for the lateral and directional cases. This recommendation is based on the observation, during the longitudinal stability flight tests, that light turbulence excited a lightly damped yawing oscillation.

3. Instrumentation be devised to investigate the short period mode as well as the lateral motions of the aircraft. Such an investigation would add completeness to the stability and control data for the Department of Aeronautics test aircraft.

4. The gain on the elevator force instrumentation amplifier be reduced. Although the force indications were usable and indeed gave reasonable results, the voltage readings were sensitive to force applications and average values often had to be used instead of steady state values.

5. The elevator force instrumentation be installed on the pilot's control wheel instead of on the copilot's wheel. This recommendation is directed at the experimental work done

at the Naval Postgraduate School where the copilot in flight testing work is generally a student who is unqualified in the aircraft. Although the copilot is generally a qualified aviator, his proficiency understandably suffers while he is serving in a nonoperational assignment. The aircraft's flight instruments, in addition, are on the pilot's side. Adoption of this recommendation would tend to reduce the time to reach steady state airspeeds, minimize excursions from those speeds, and minimize repetitive testing.

6. Flight theses be projects for two students working in concert on the same investigation. Since multi-engine aircraft normally require two pilots, two researchers co-investigating a topic would permit ease of flight scheduling, would reduce the time required for experimental design, and would permit a more rapid rate of data acquisition.



Figure 1
CESSNA 310H AIRCRAFT N164X

Appendix A
Figures

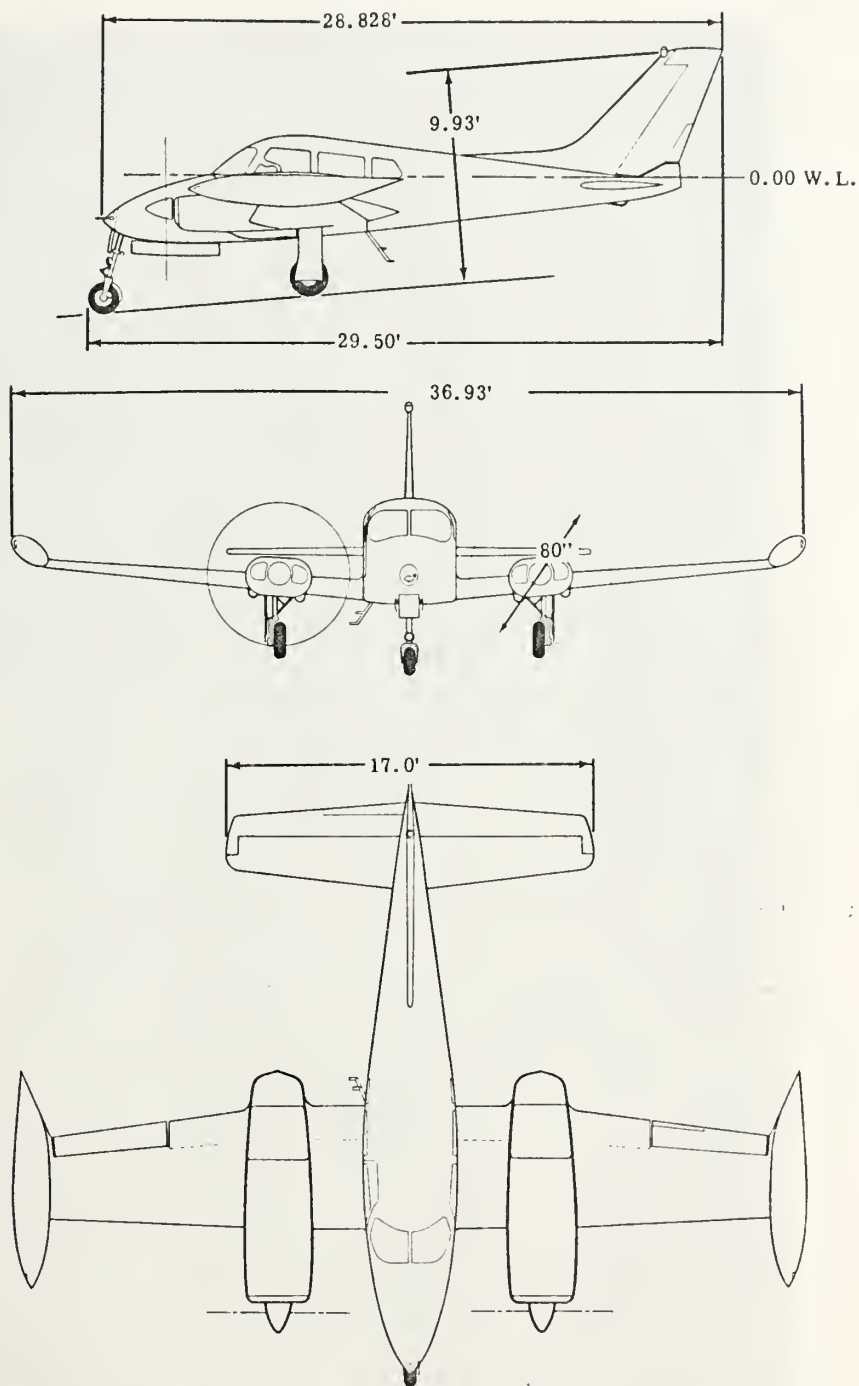


Figure 2

CESSNA 310H DIMENSIONS

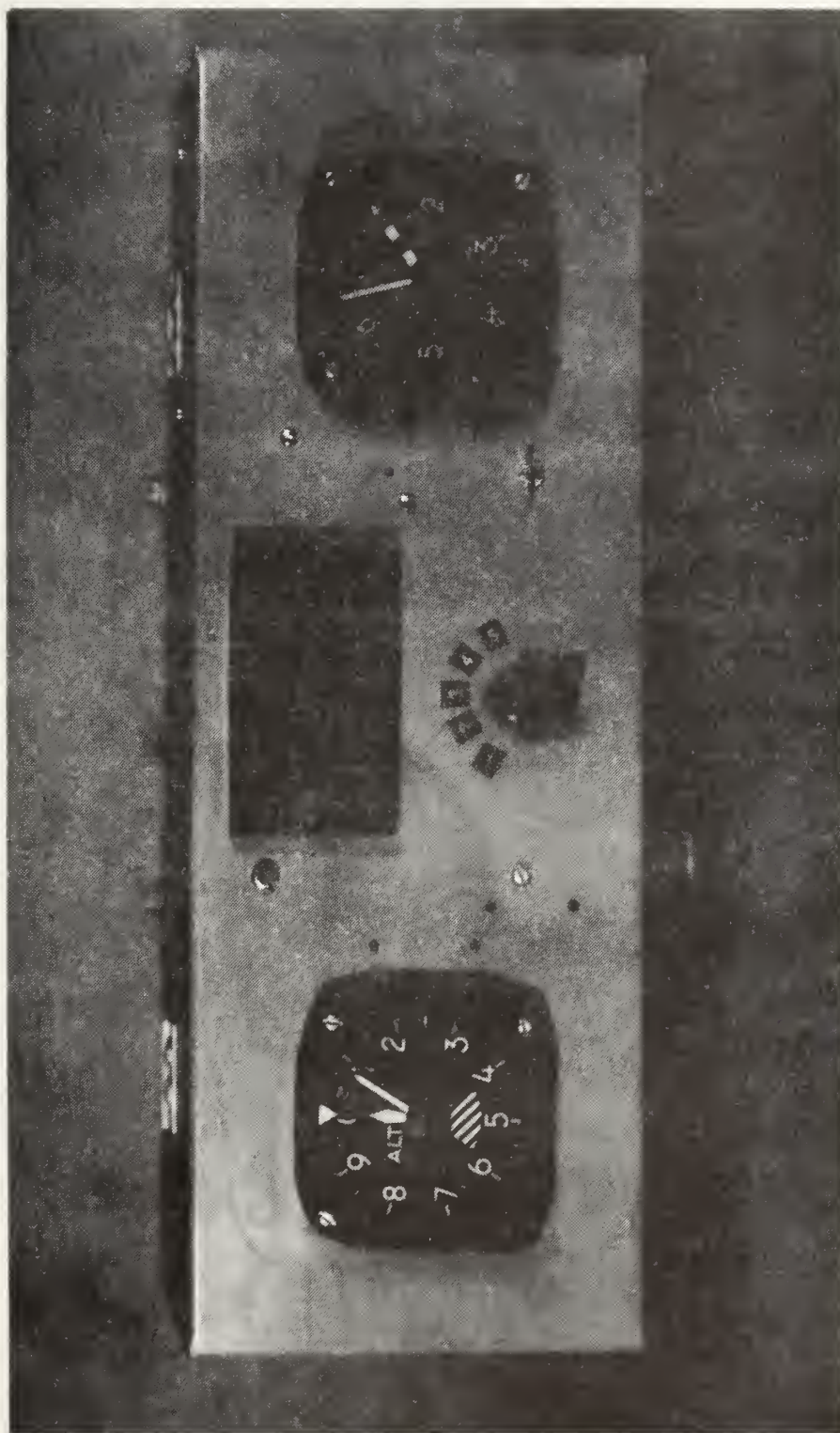


Figure 3
INSTRUMENT CONSOLE

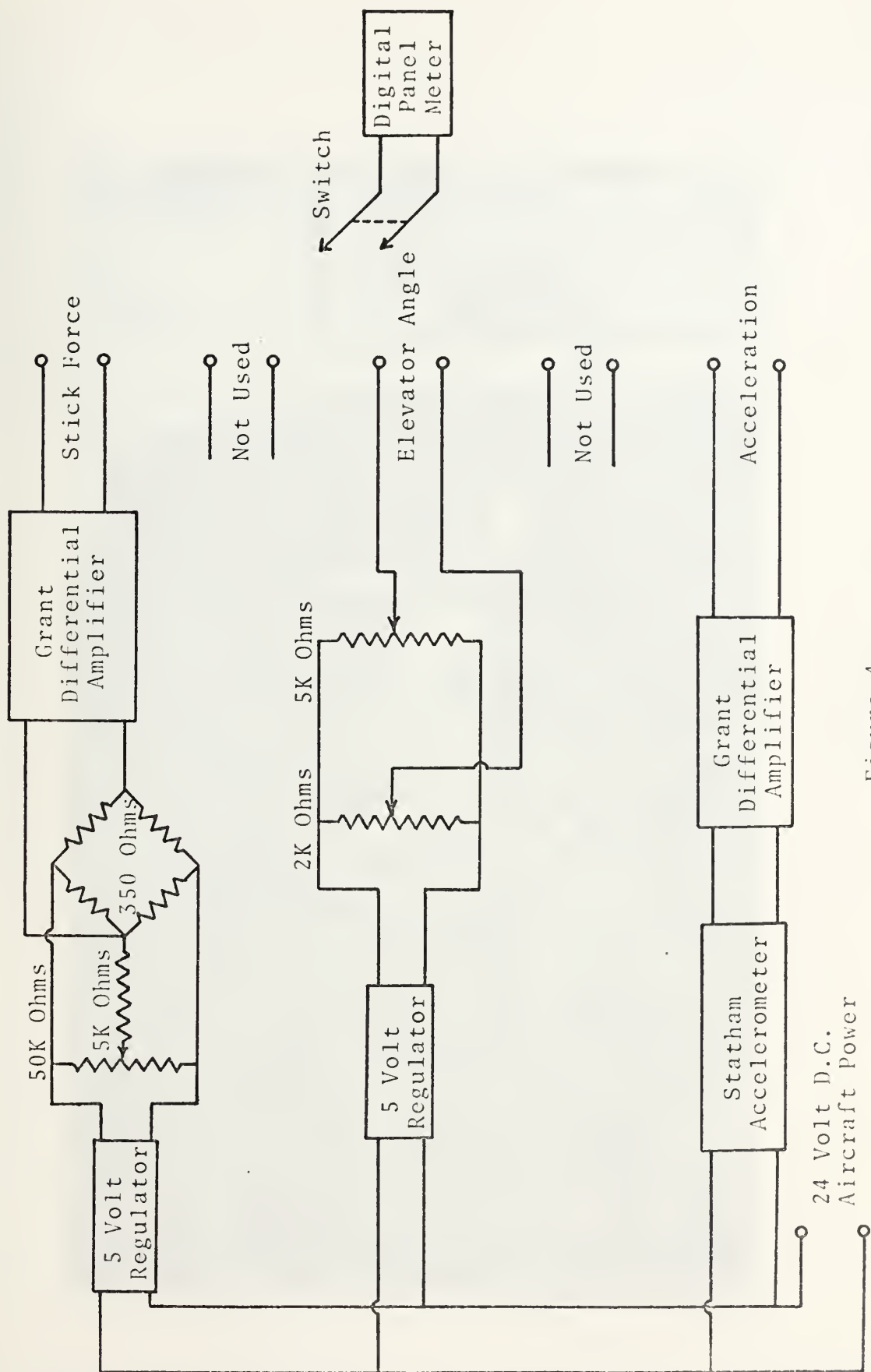


Figure 4

INSTRUMENTATION SYSTEM

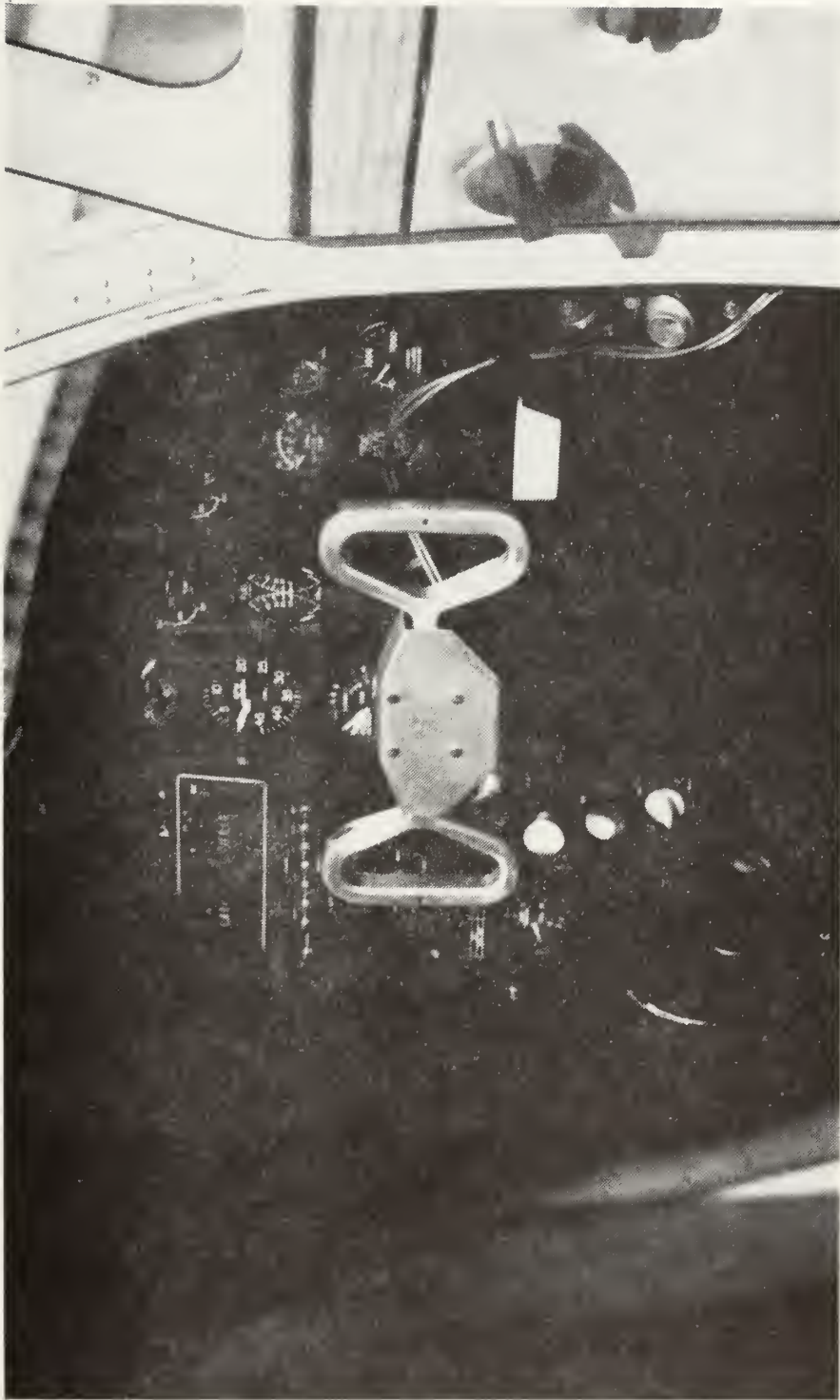


Figure 5
FORCE MEASURING WHEEL

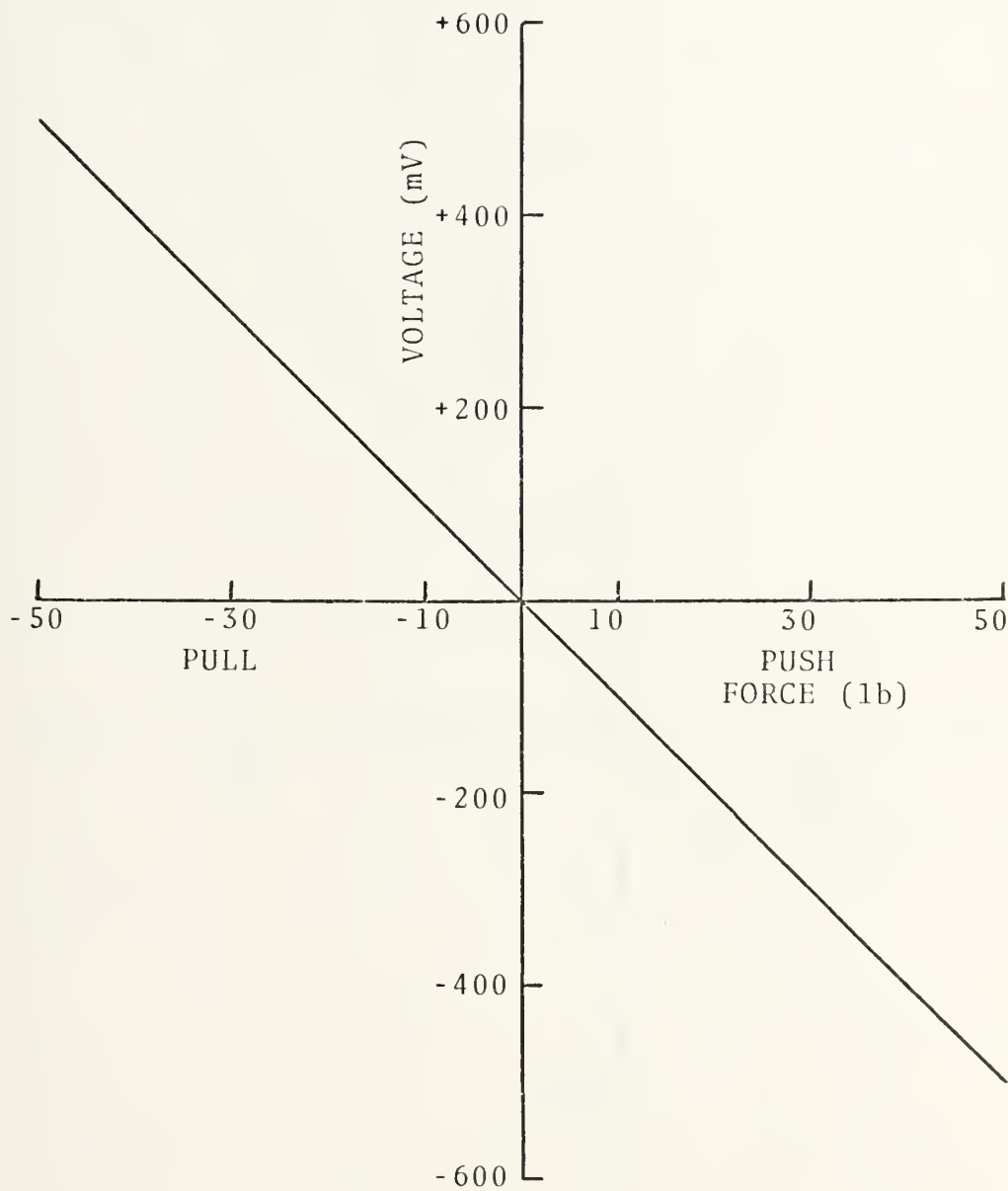


Figure 6
ELEVATOR FORCE CALIBRATION

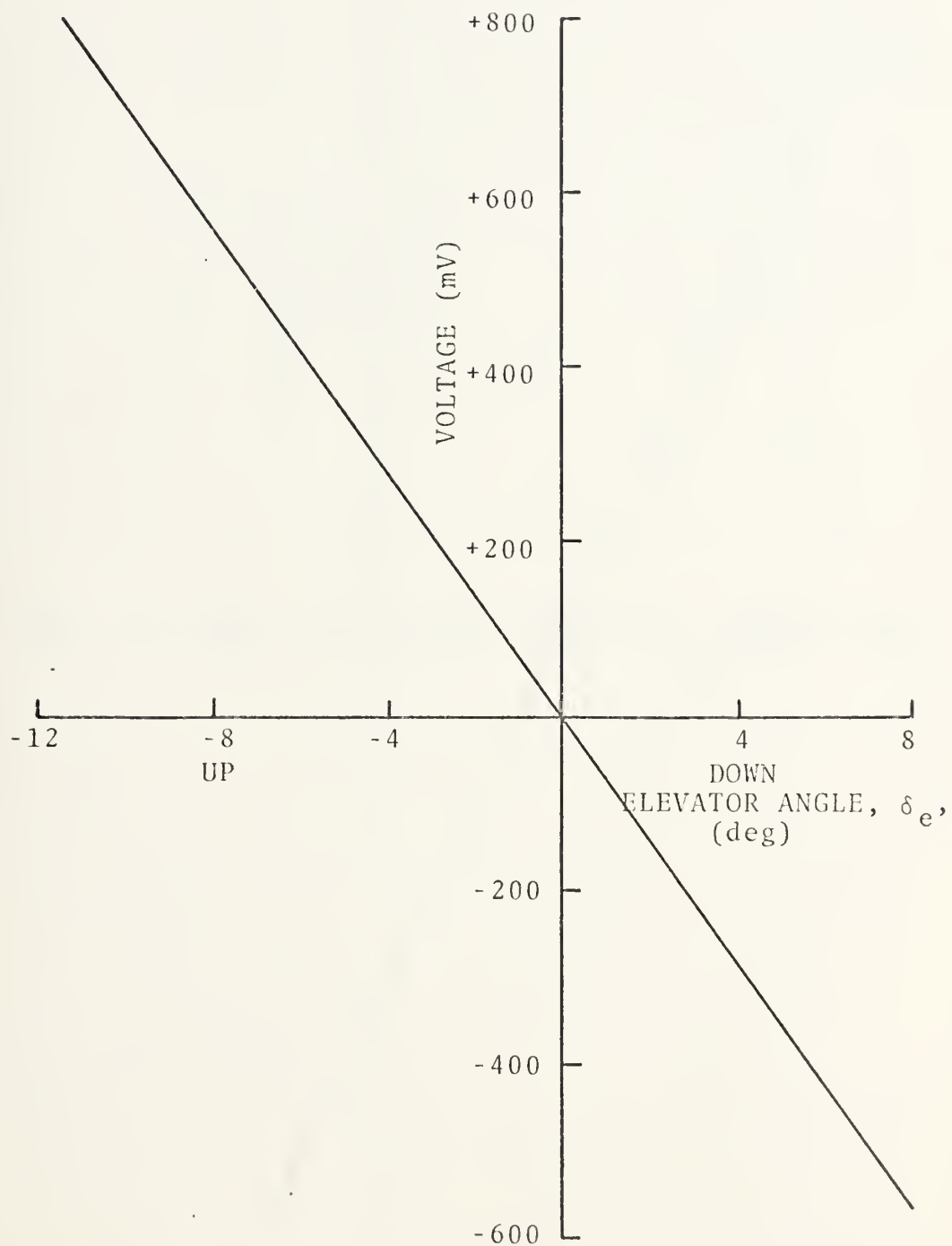


Figure 7
ELEVATOR POSITION CALIBRATION

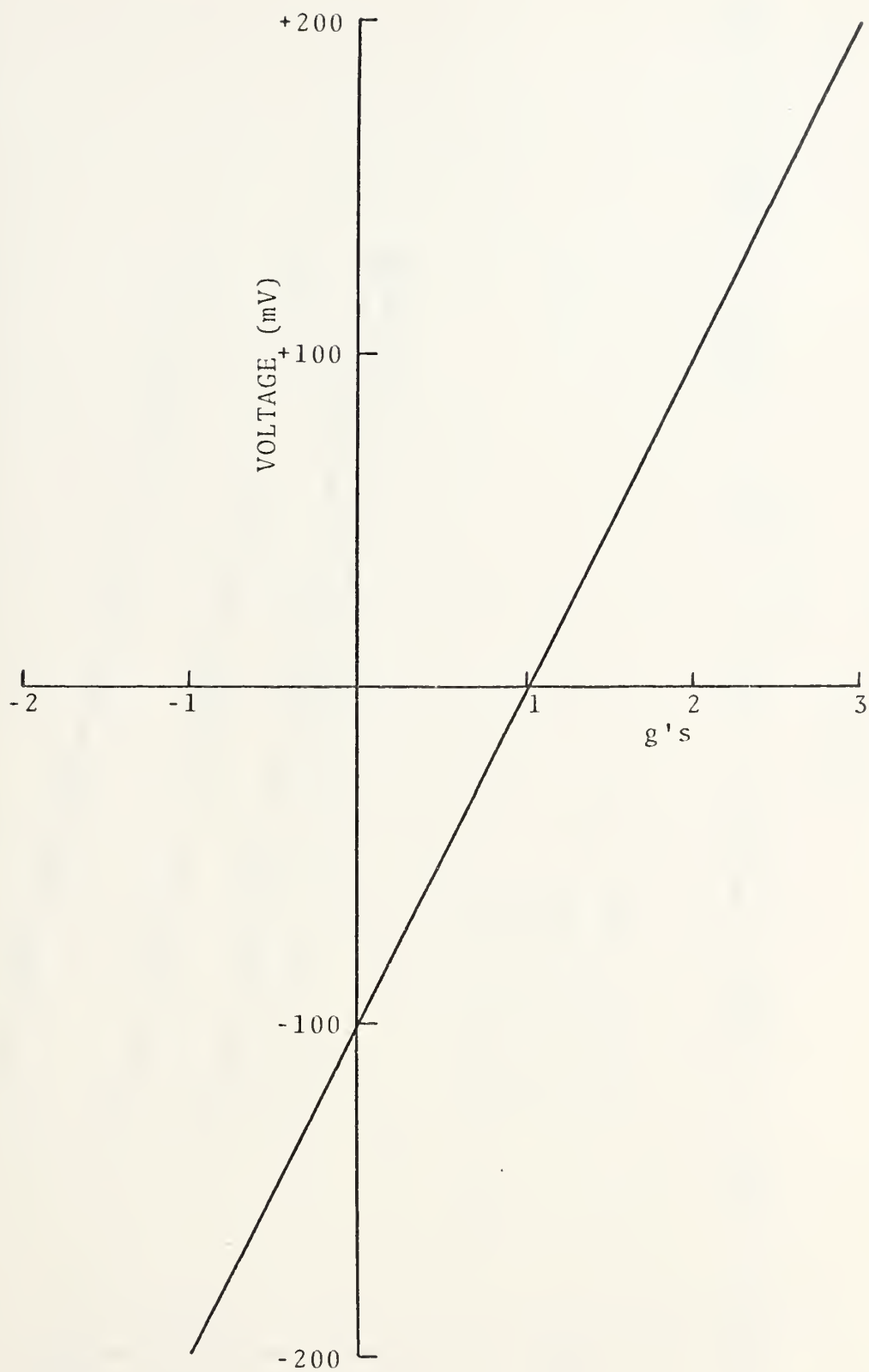


Figure 8
ACCELEROMETER CALIBRATION

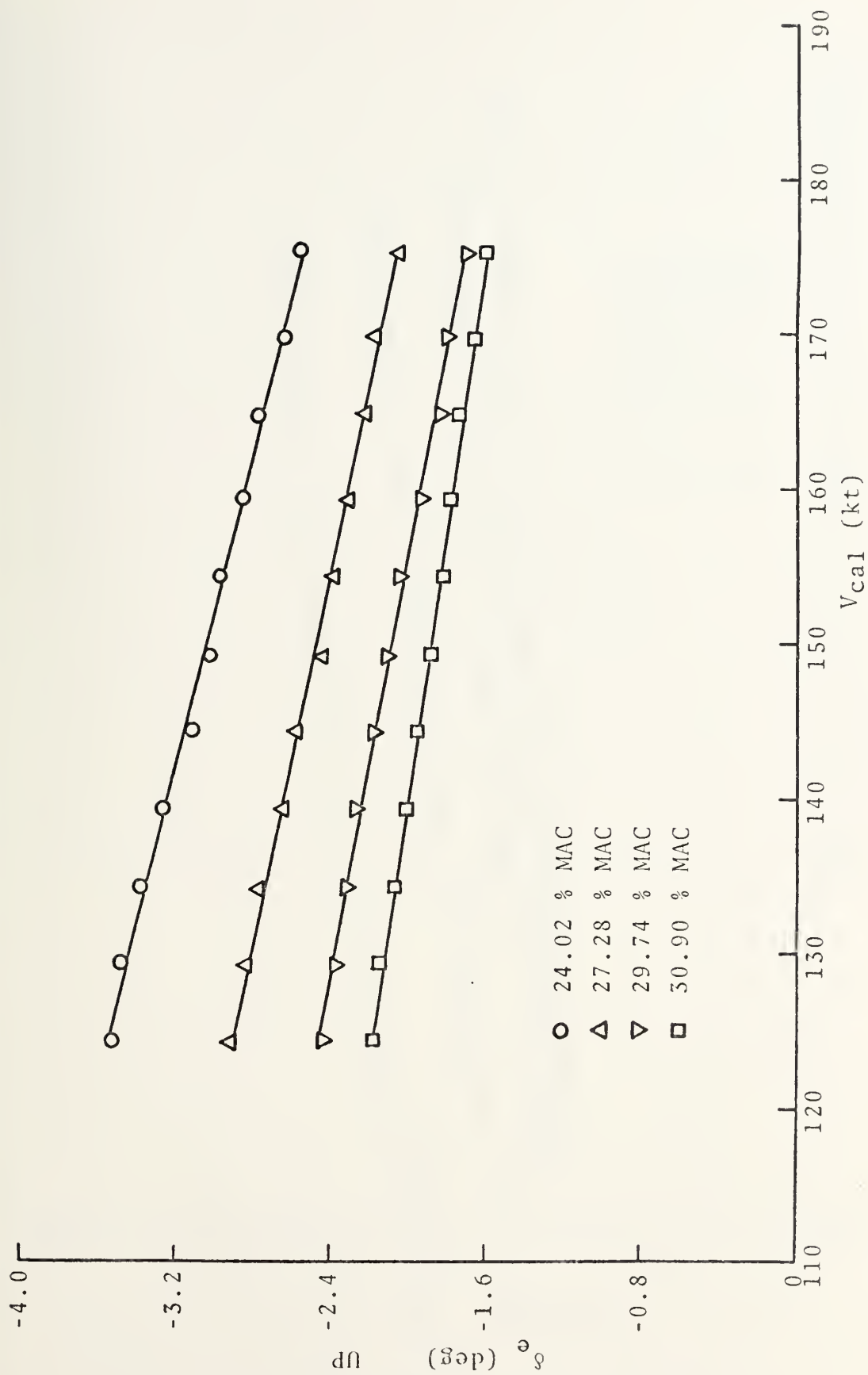


Figure 9
CRUISE CONFIGURATION
 δ_c vs. V_{cal}

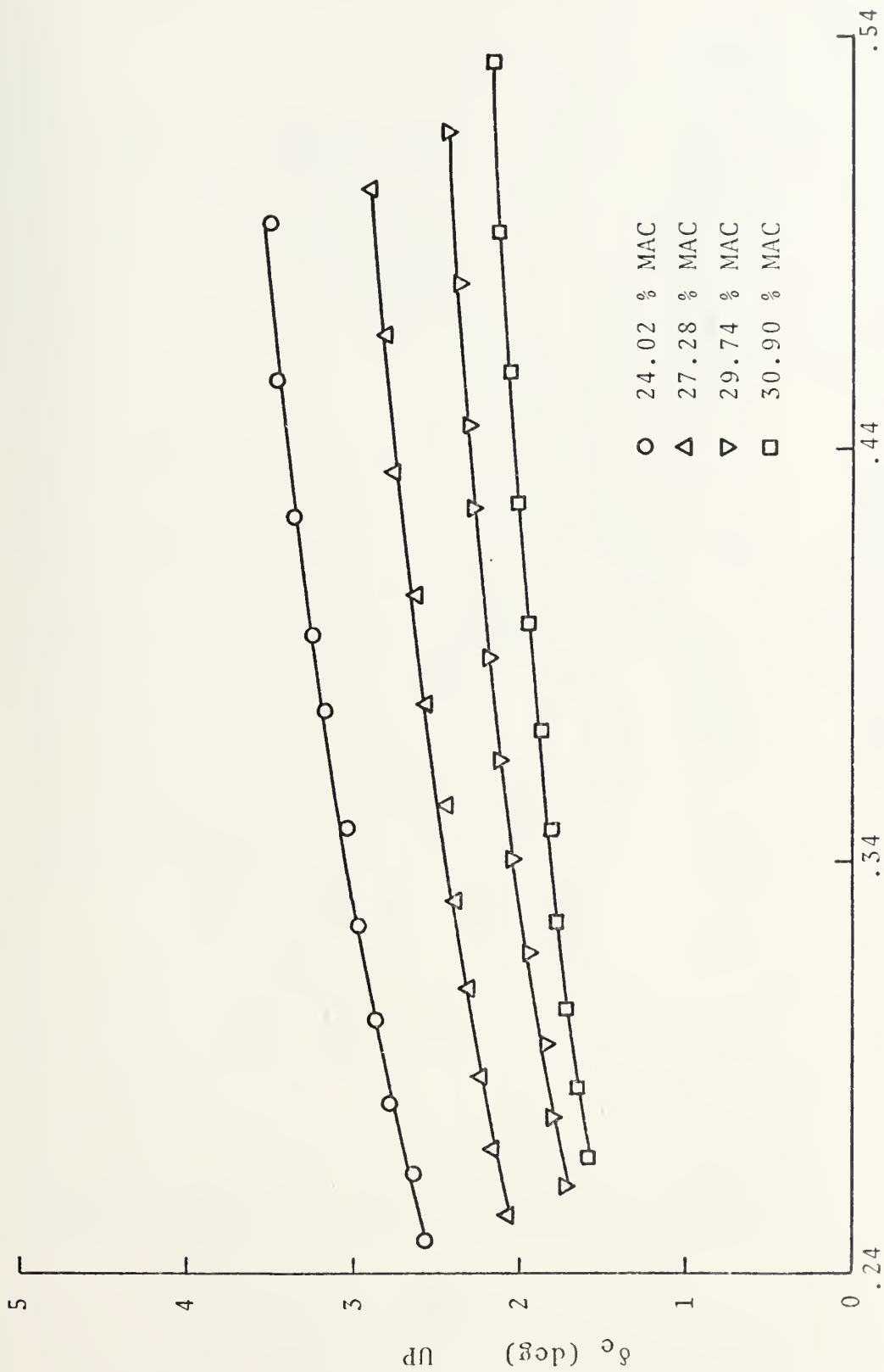


Figure 10
CRUISE CONFIGURATION
 δ_e vs. C_L

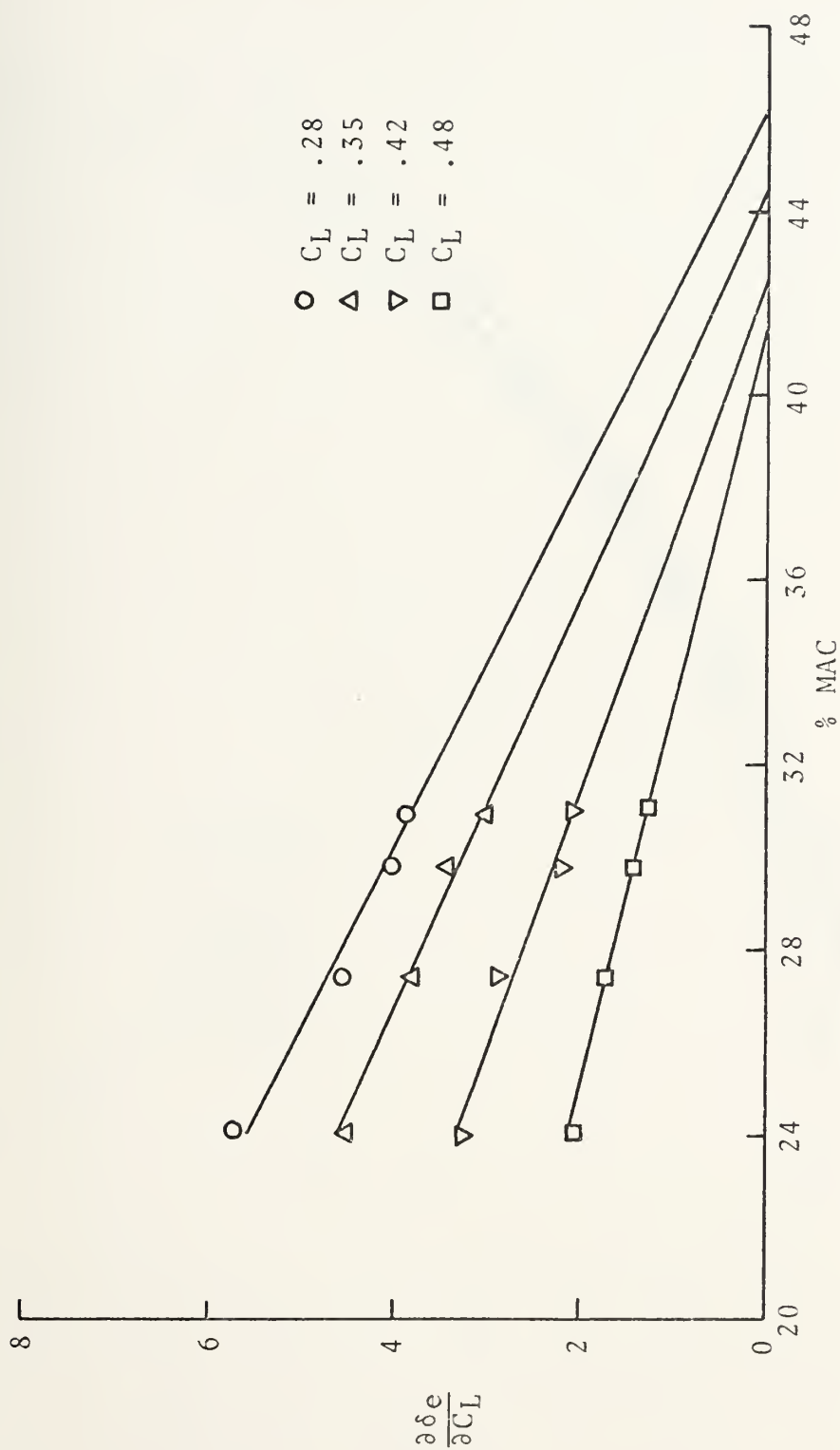


Figure 11
CRUISE CONFIGURATION

$$\frac{\partial \delta e}{\partial C_L} \text{ vs. } \% \text{ MAC}$$

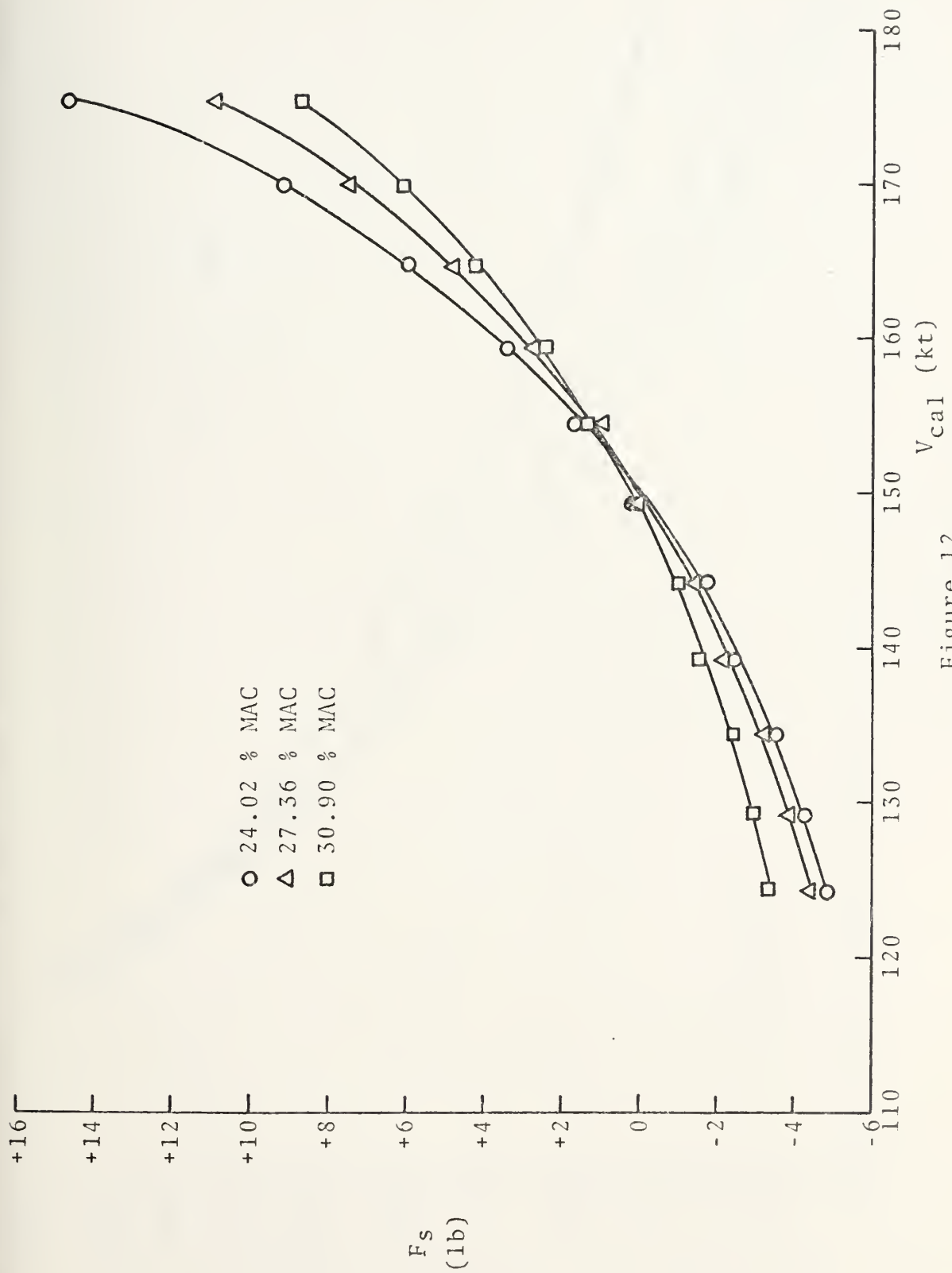


Figure 12
CRUISE CONFIGURATION
 F_s vs. V_{cal}

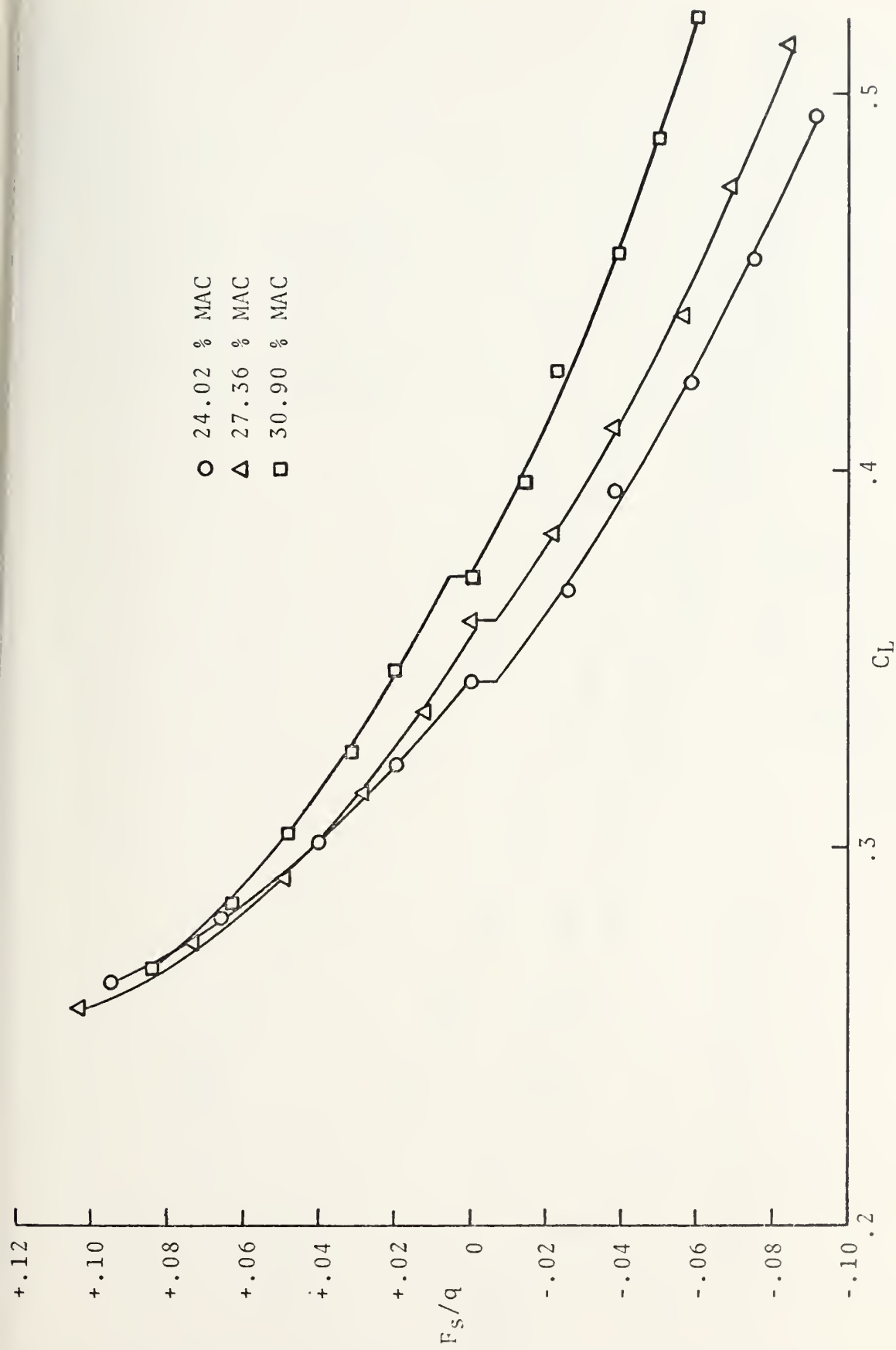


Figure 13
CRUISE CONFIGURATION
 F_s/q vs. C_L

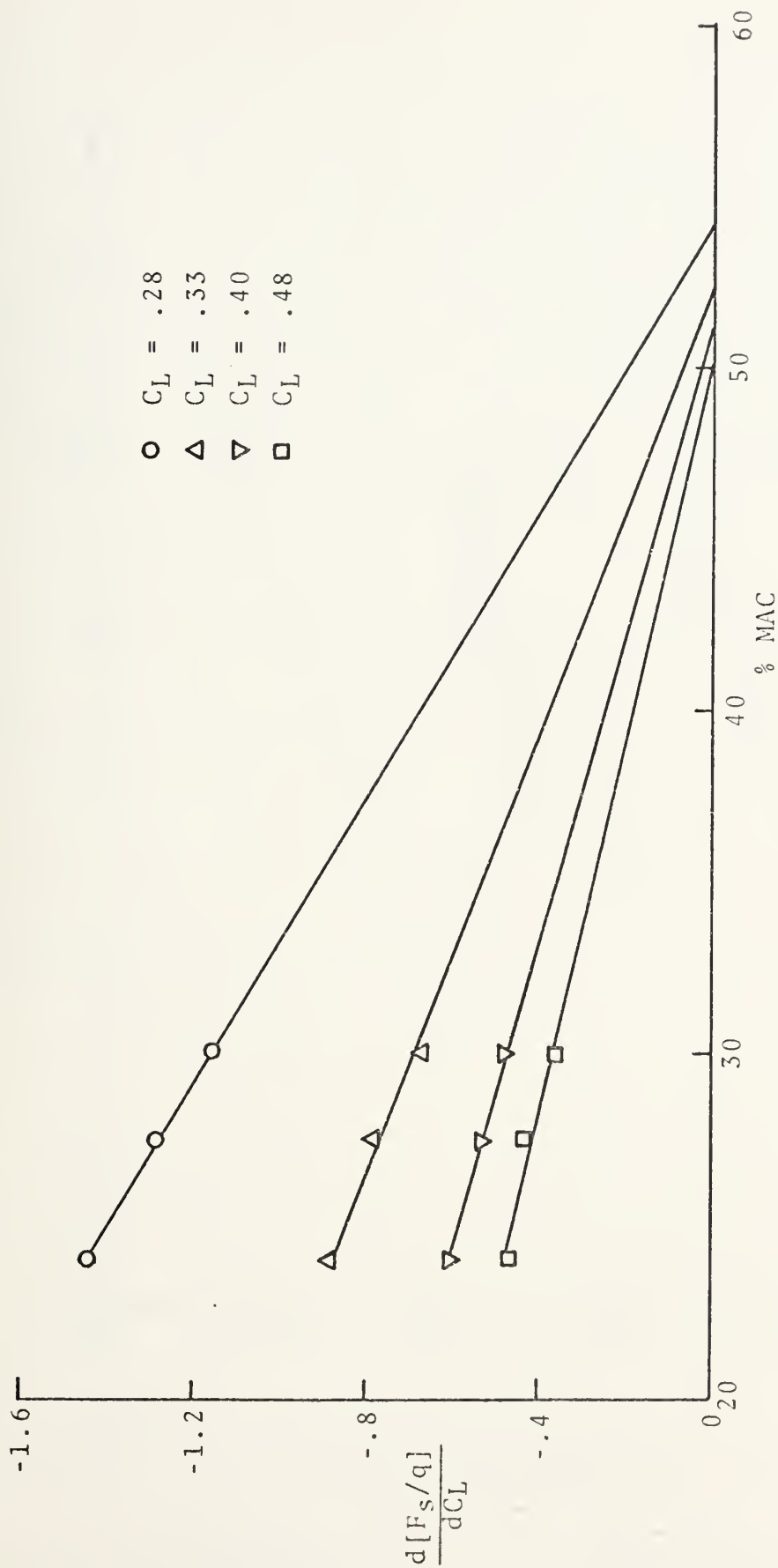


Figure 14
CRUISE CONFIGURATION
 $\frac{d[F_s/q]}{dC_L}$ vs. % MAC

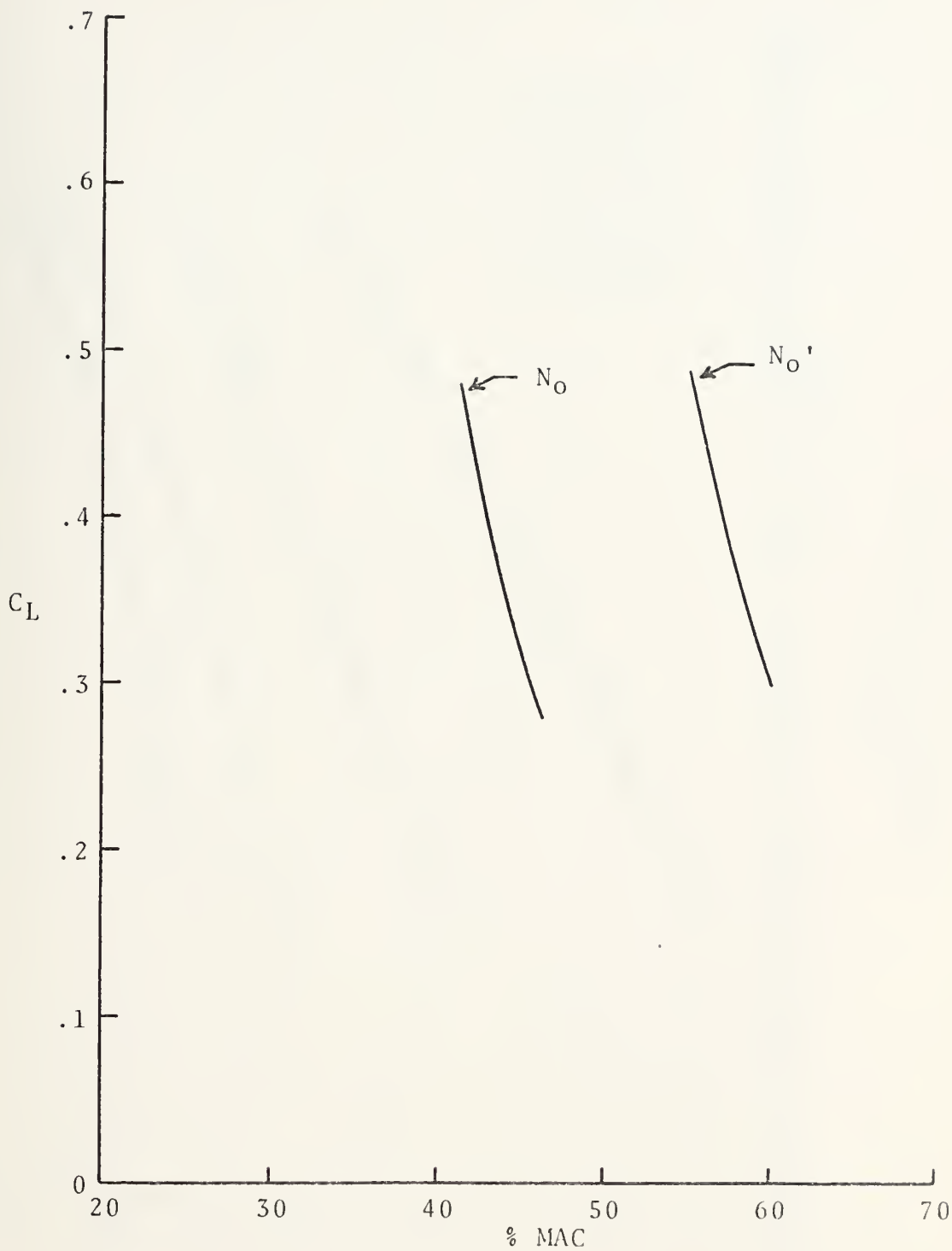


Figure 15
CRUISE CONFIGURATION
 N_O and N_O' vs. C_L

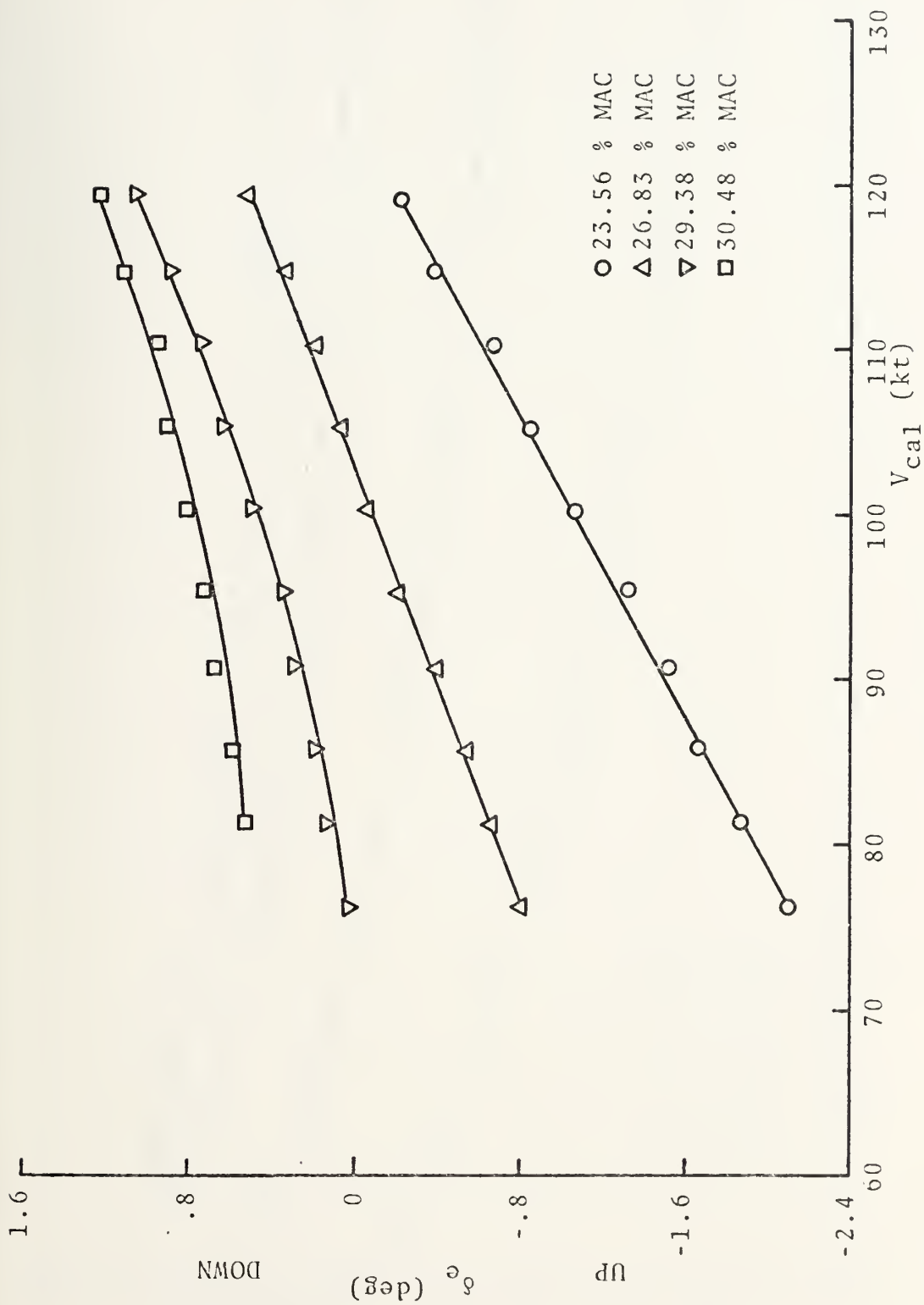


Figure 16
 APPROACH CONFIGURATION
 δ_c vs. V_{cal}

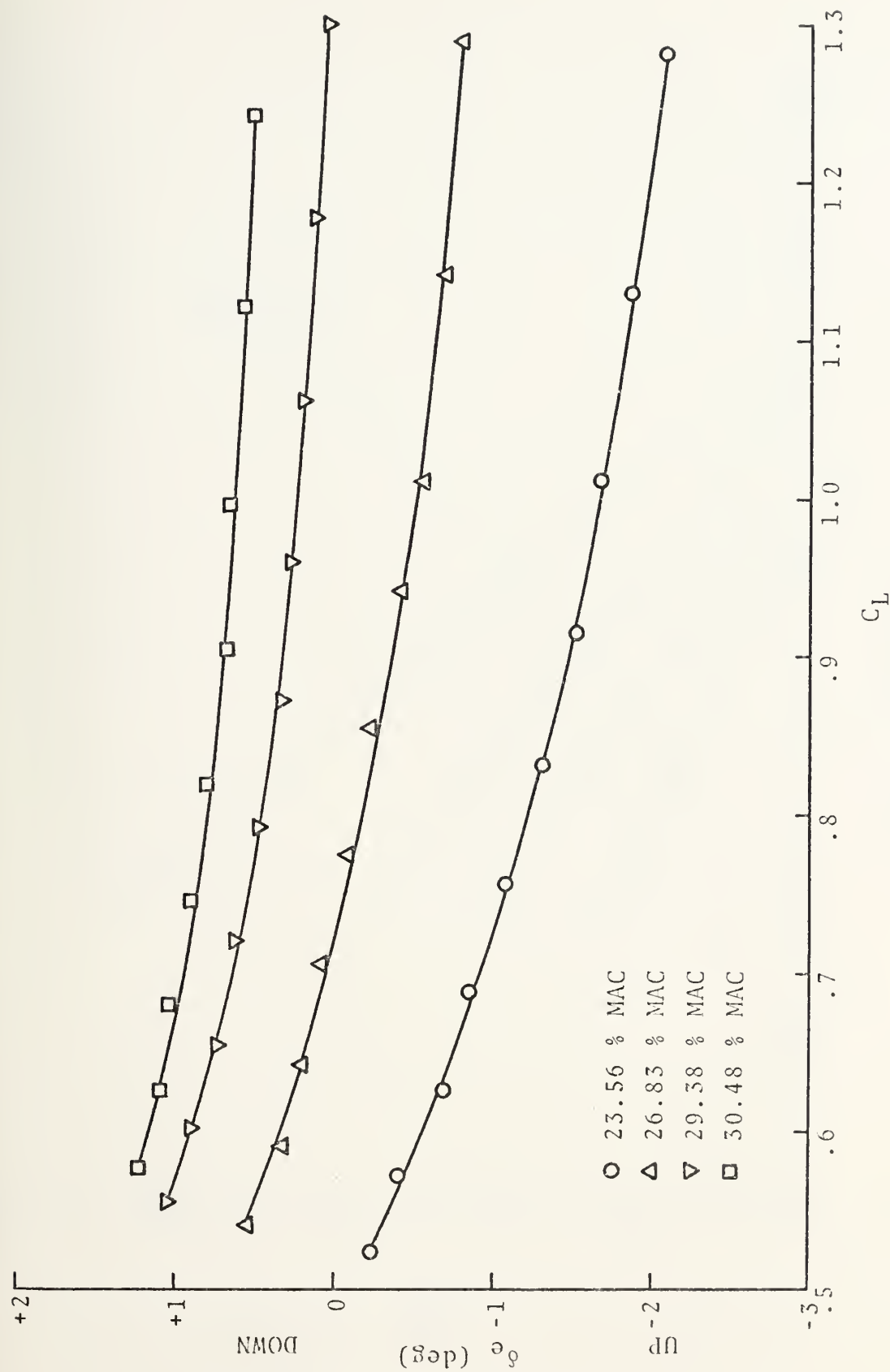


Figure 17

APPROACH CONFIGURATION

δ_e vs. C_L

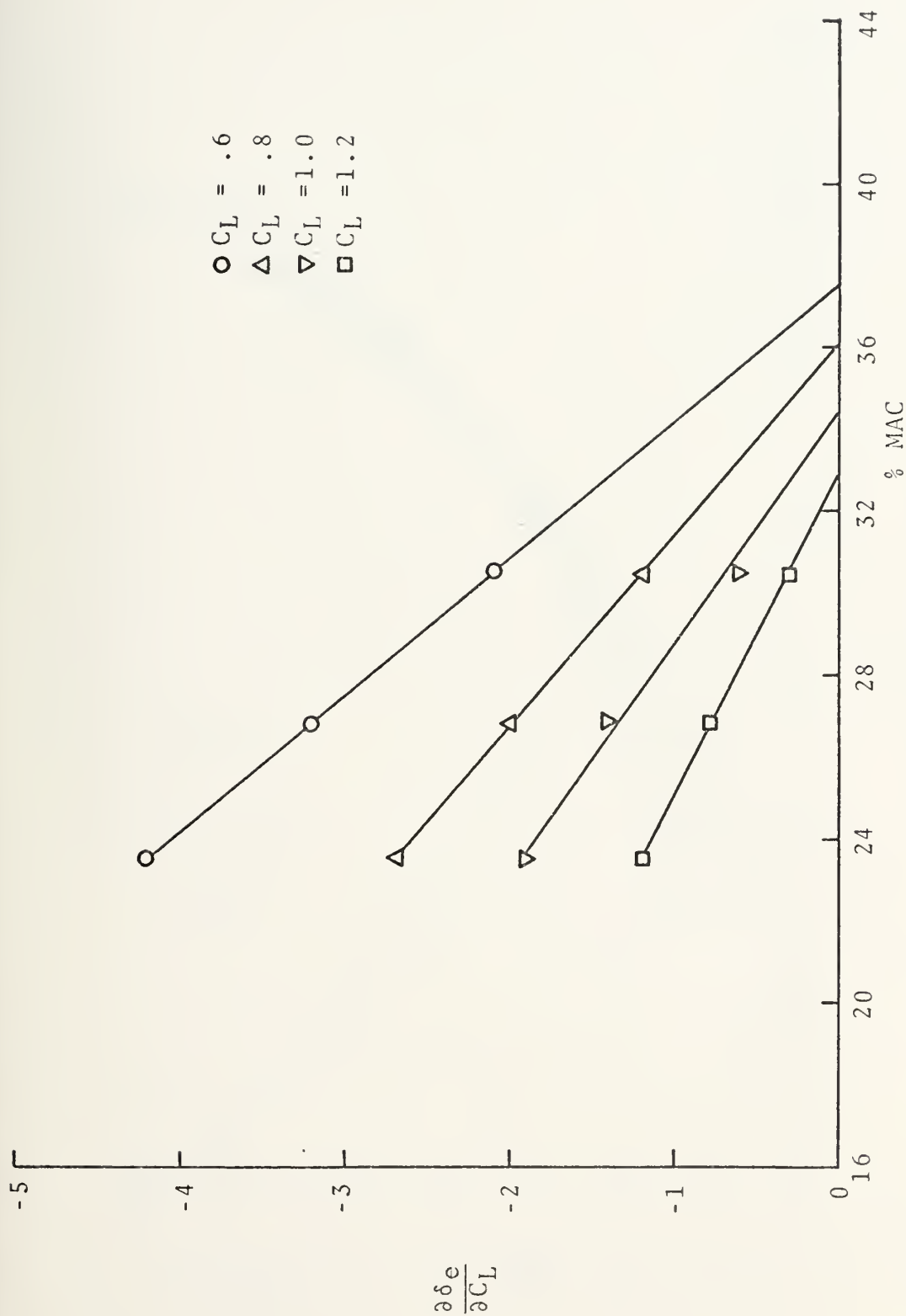


Figure 18

APPROACH CONFIGURATION

$\frac{\partial \delta e}{\partial C_L}$ vs. % MAC

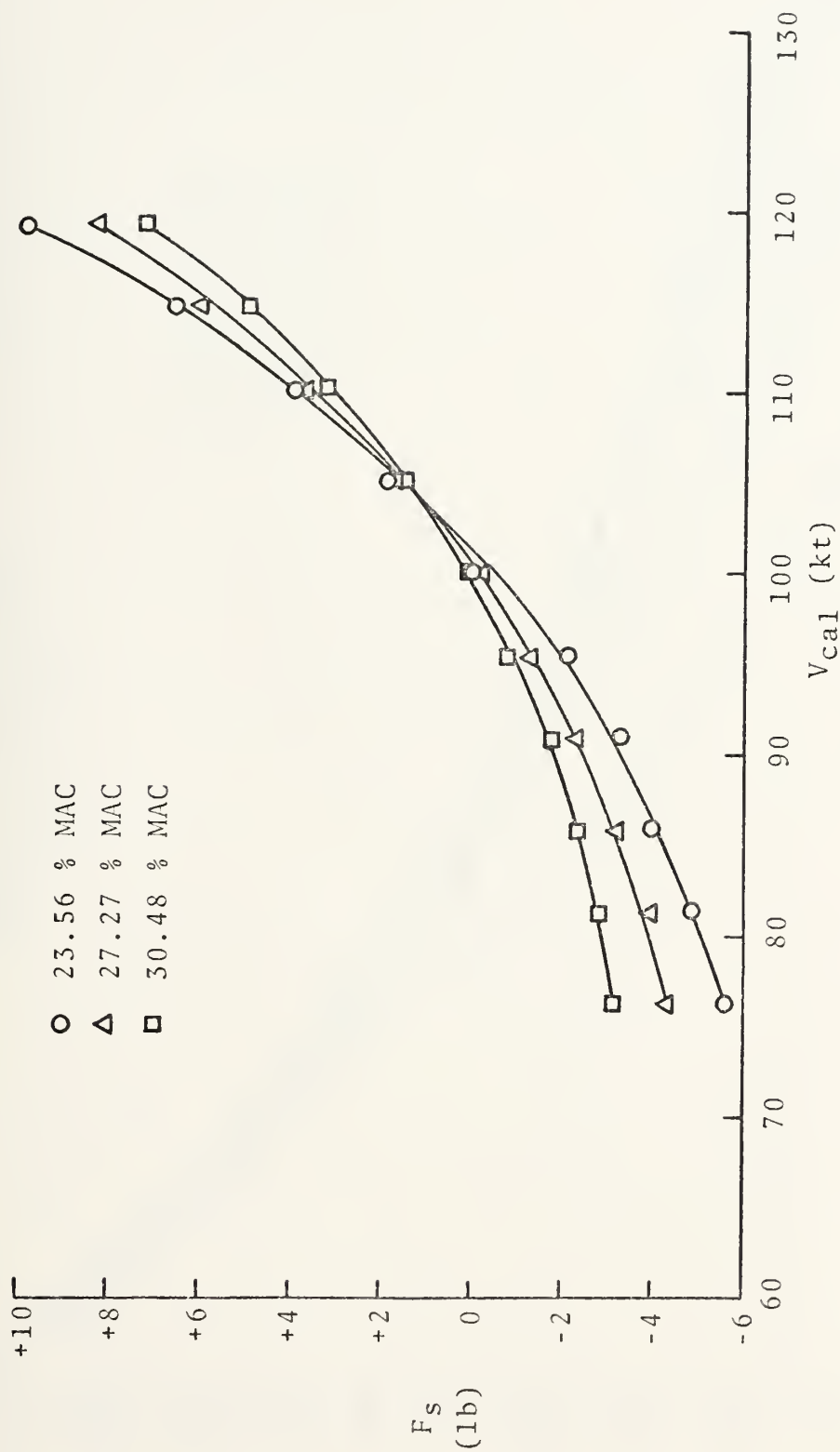
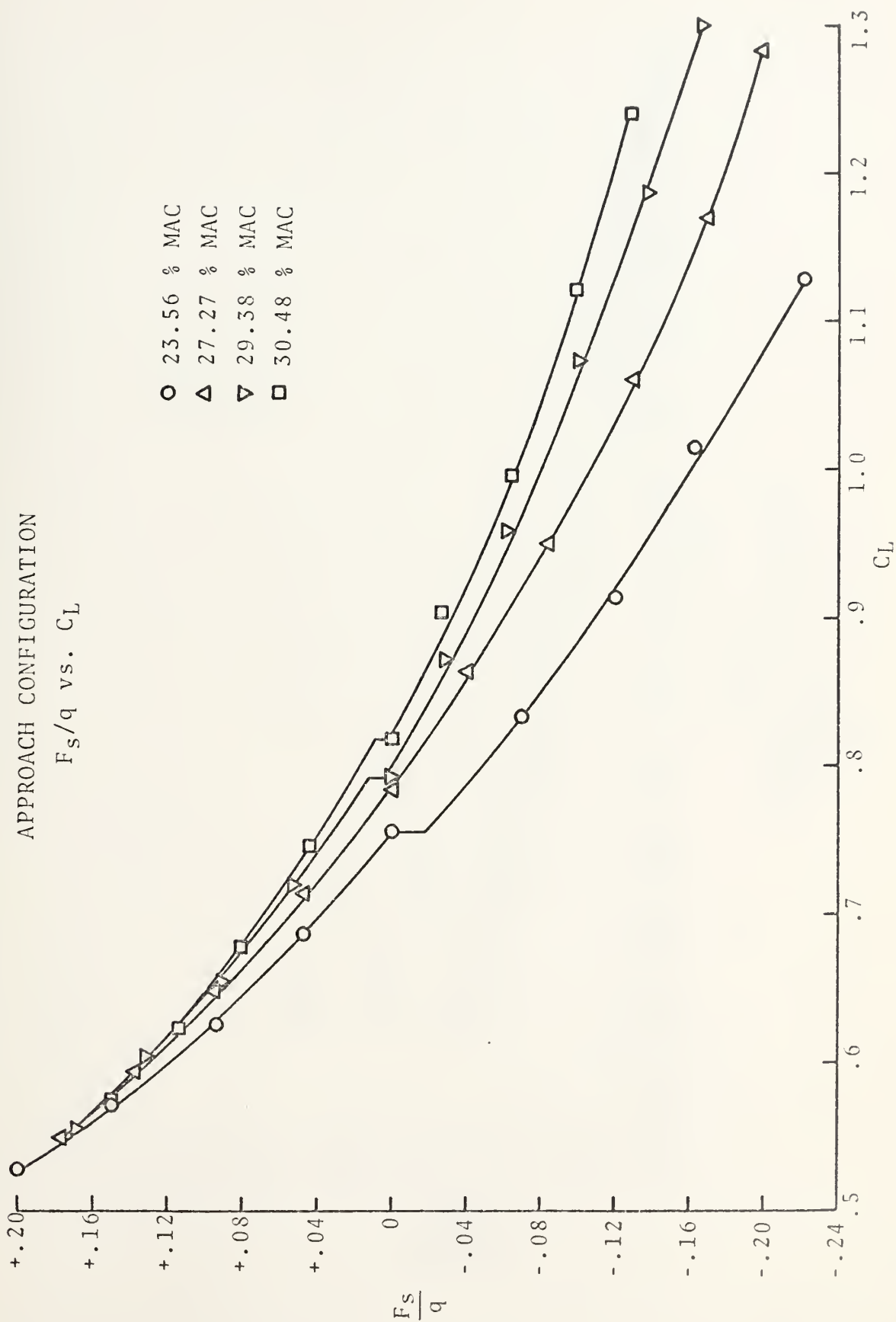


Figure 19
APPROACH CONFIGURATION
 F_s vs. V_{cal}

Figure 20



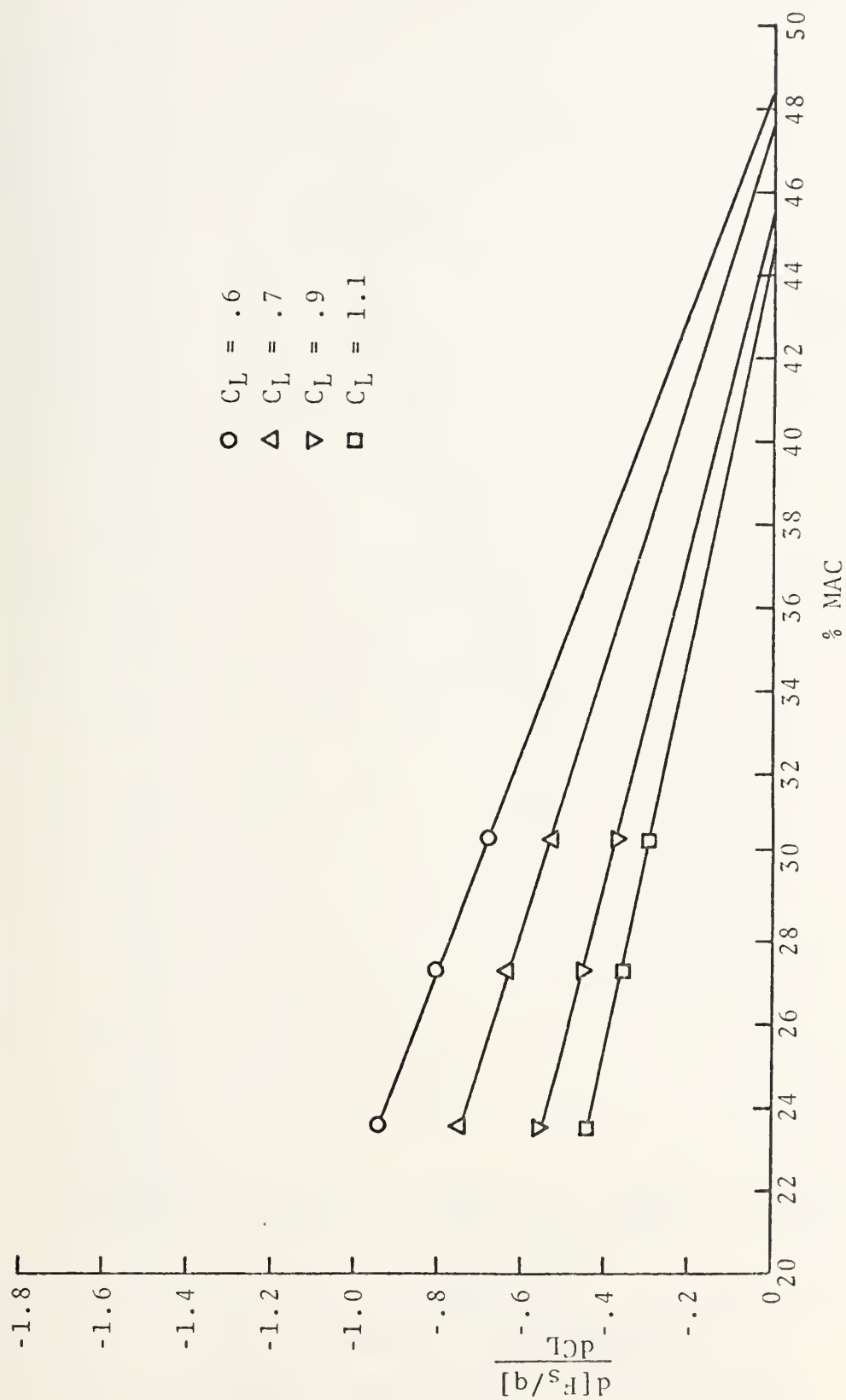


Figure 21

APPROACH CONFIGURATION

$$\frac{d[F_s/q]}{dC_L} \text{ vs. } \% \text{ MAC}$$

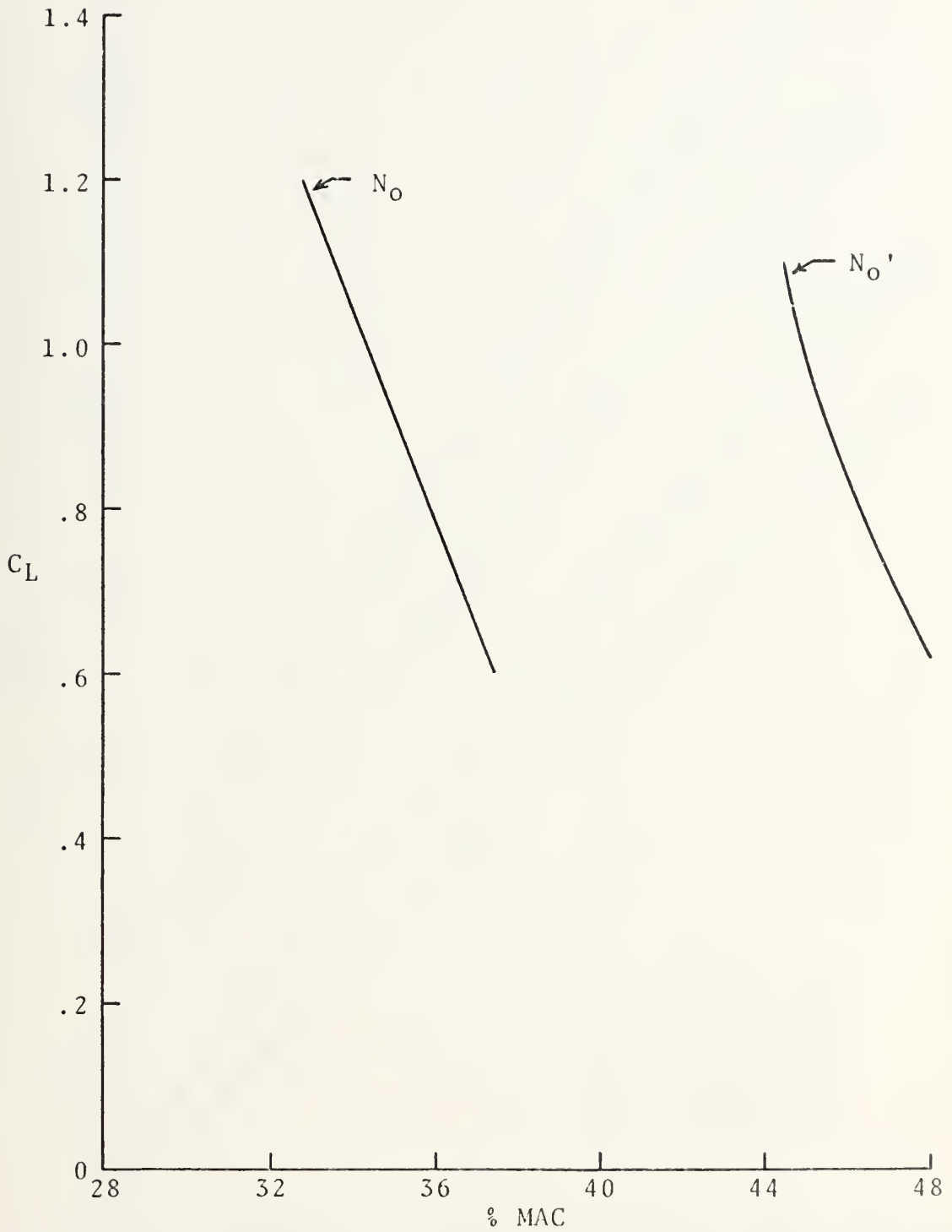


Figure 22
APPROACH CONFIGURATION
 N_O and N_O' vs. C_L

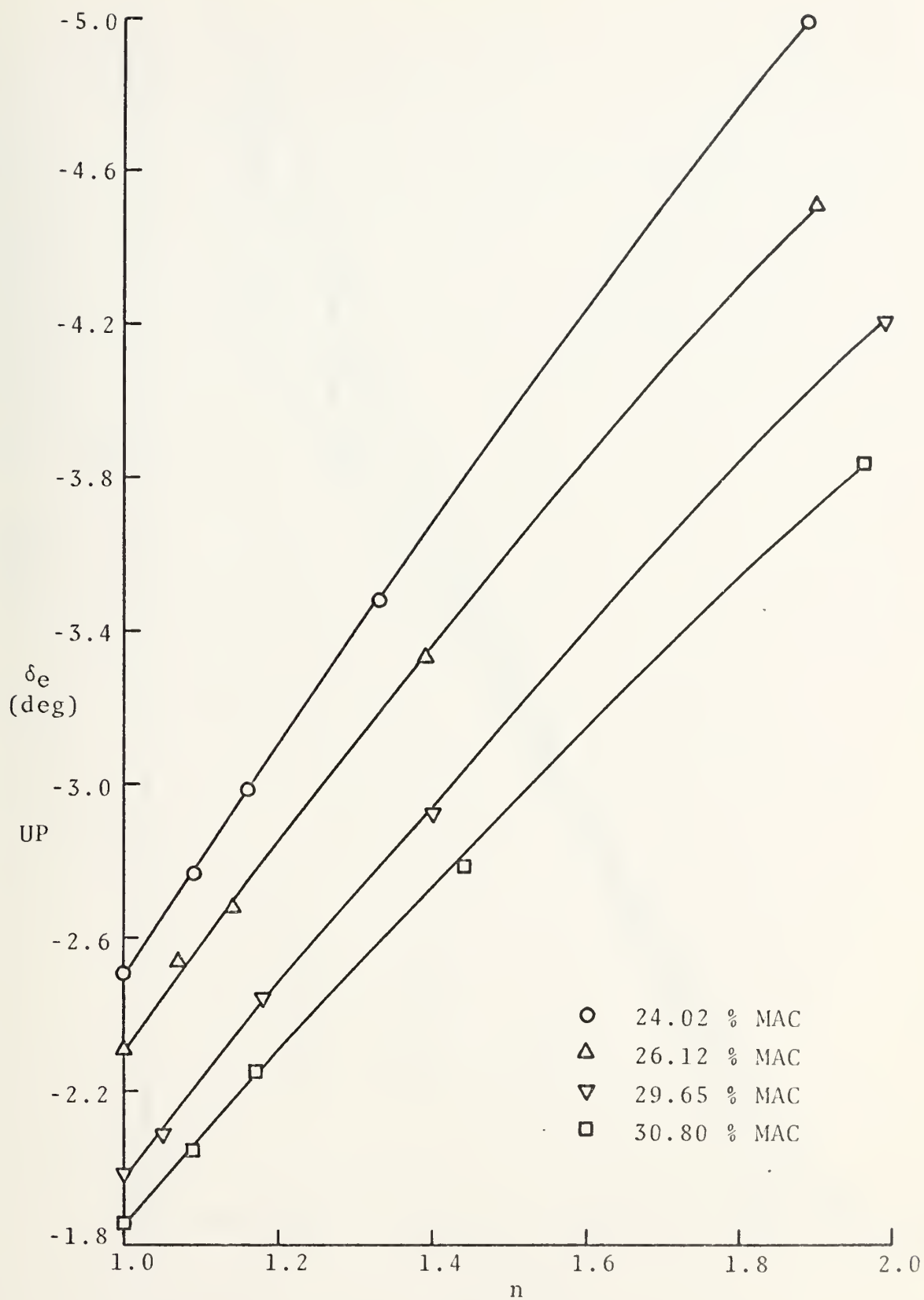


Figure 23
CRUISE CONFIGURATION
 δ_e vs. n

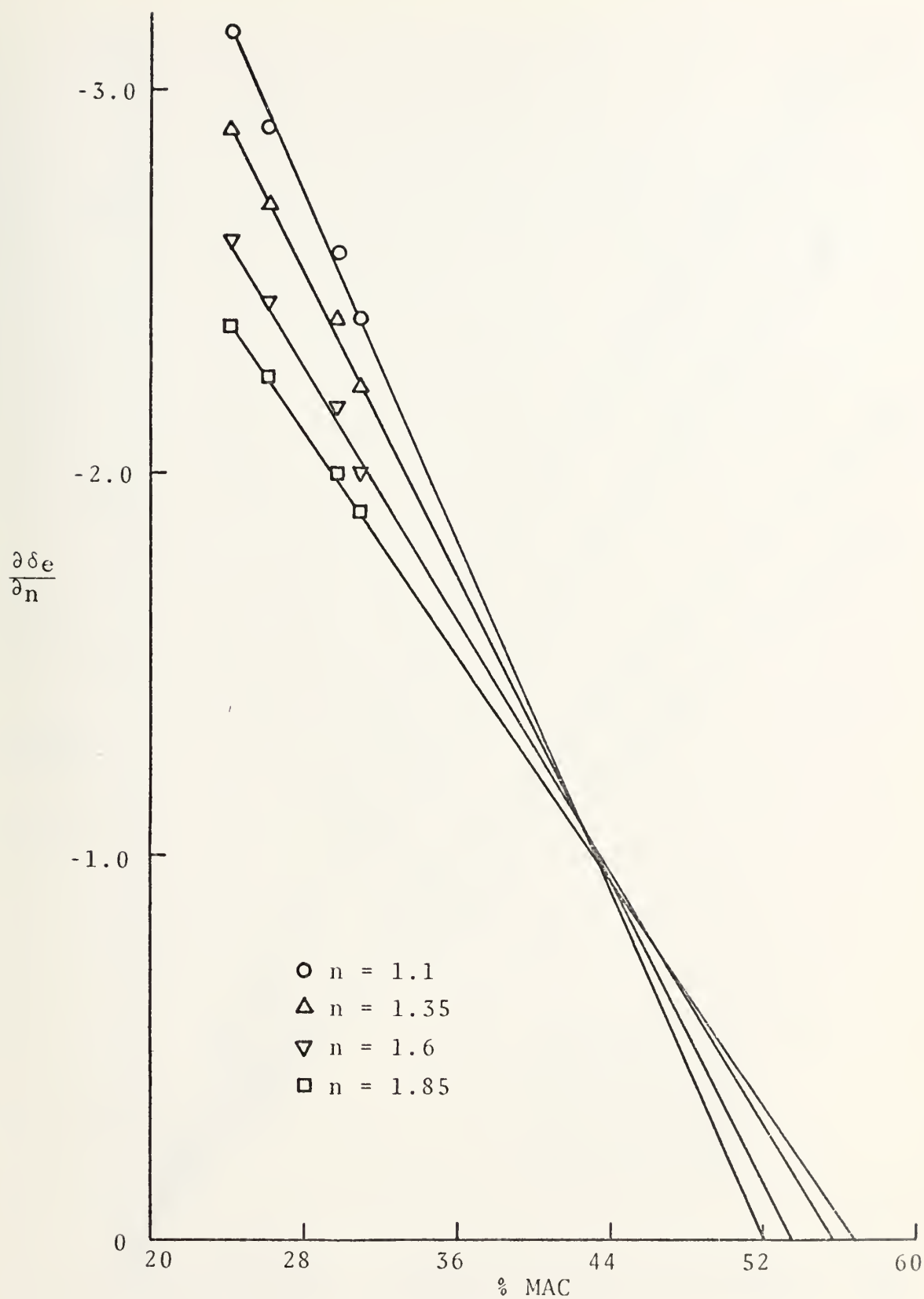


Figure 24
CRUISE CONFIGURATION

$\frac{\partial \delta_e}{\partial n}$ vs. % MAC

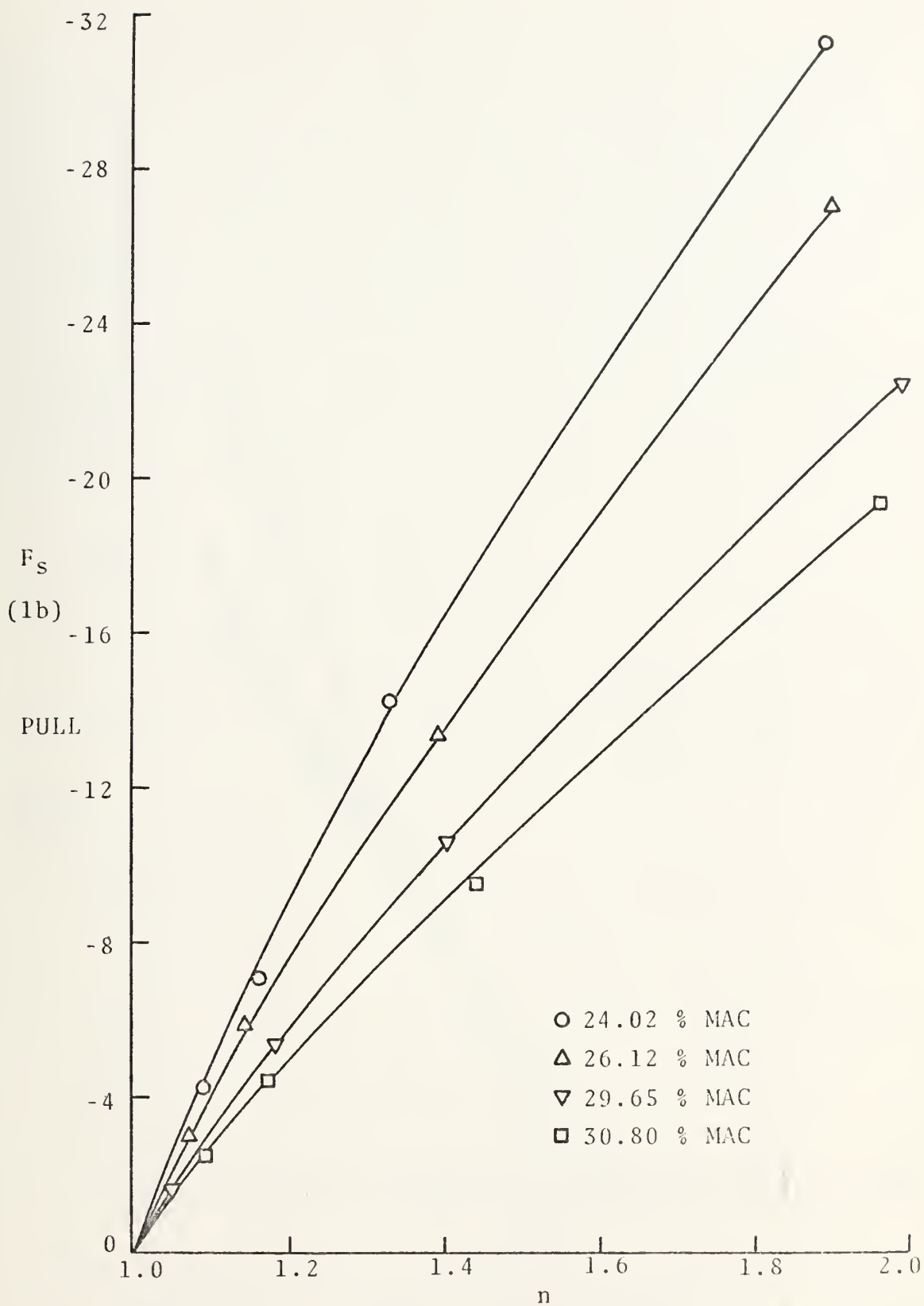


Figure 25
CRUISE CONFIGURATION
 F_S vs. n

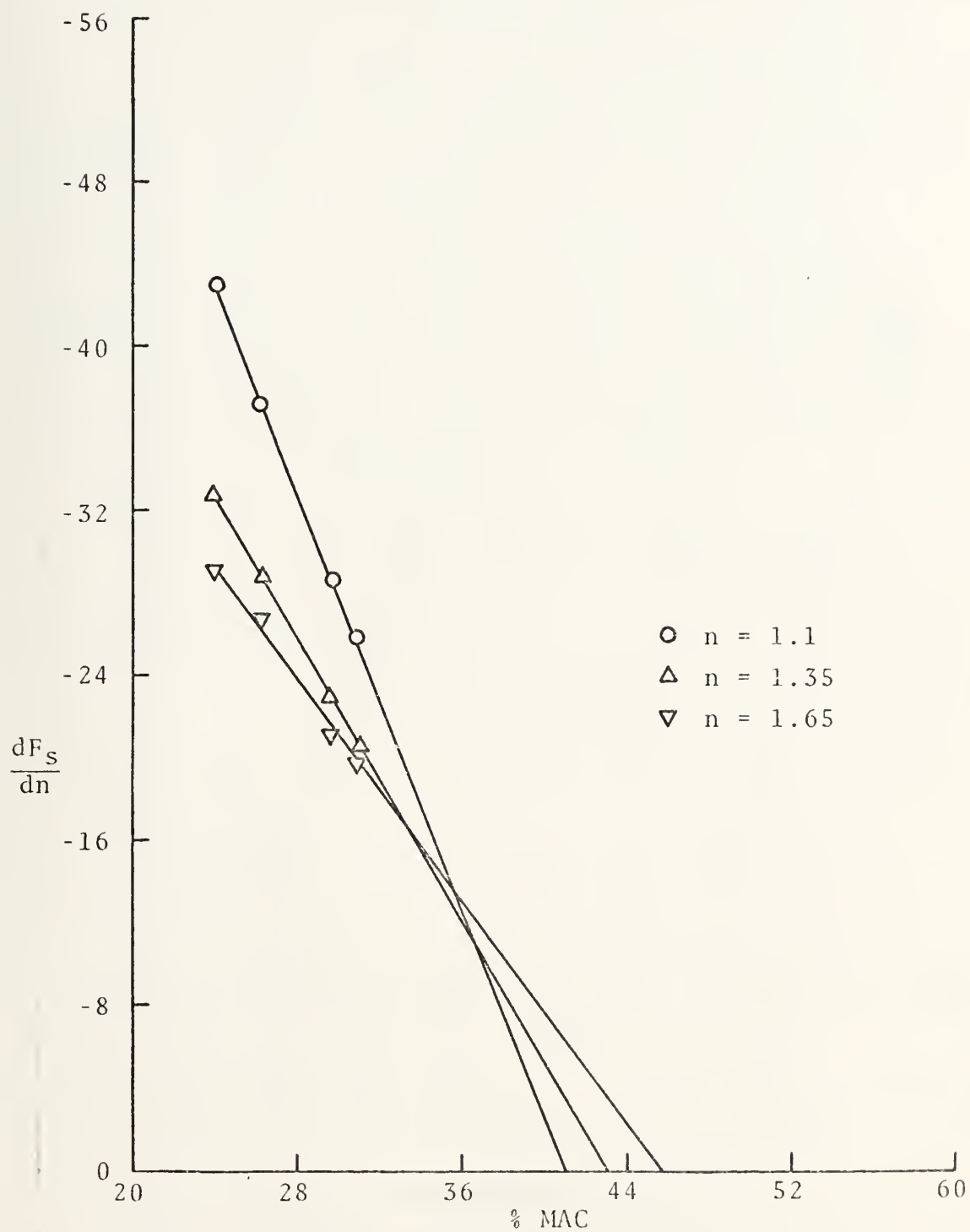


Figure 26
CRUISE CONFIGURATION
 $\frac{dF_s}{dn}$ vs. % MAC

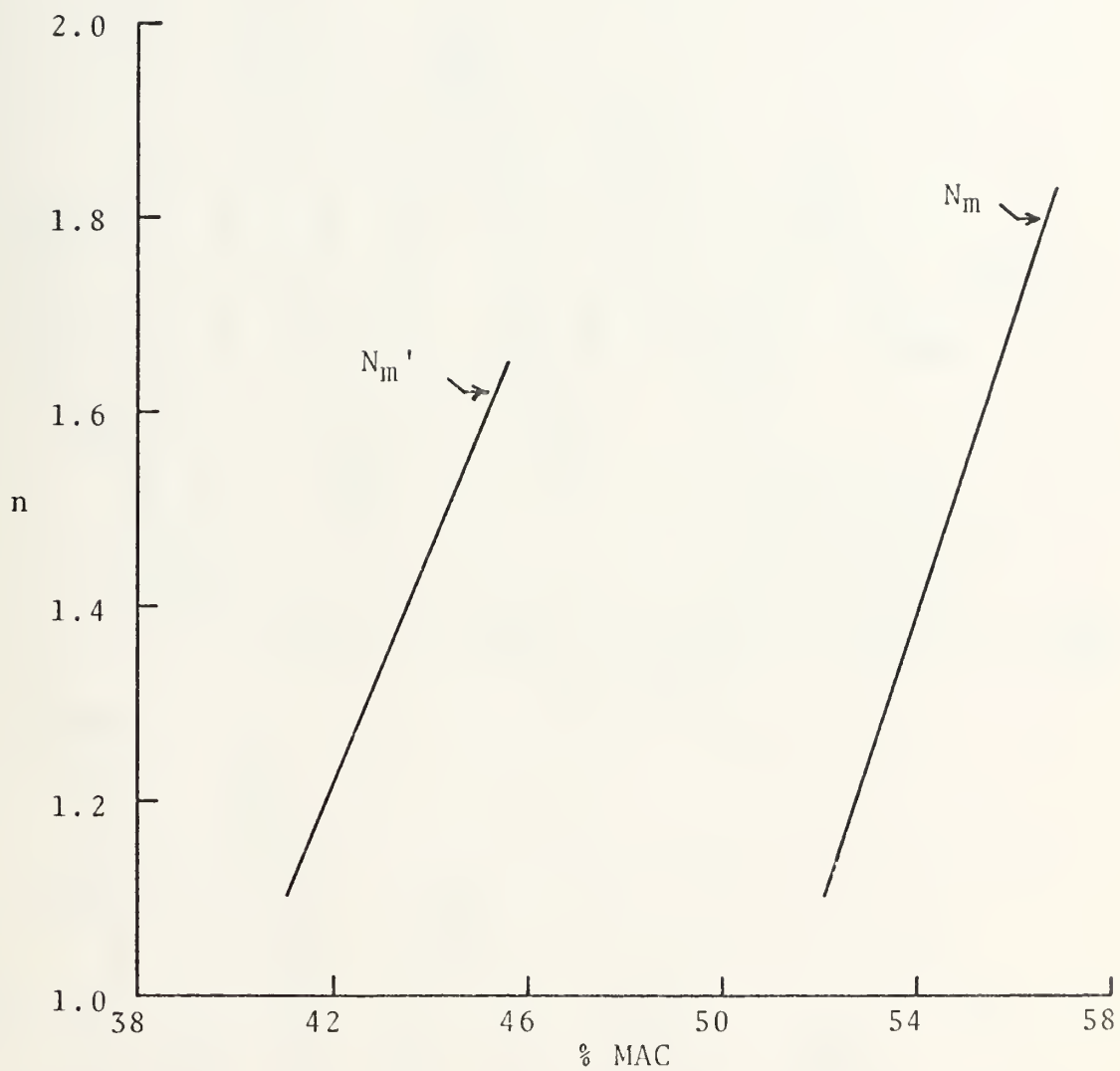


Figure 27
CRUISE CONFIGURATION
 N_m and N_m' vs. n

Figure 28
PHUGOID CHARACTERISTICS
CONTROLS FREE

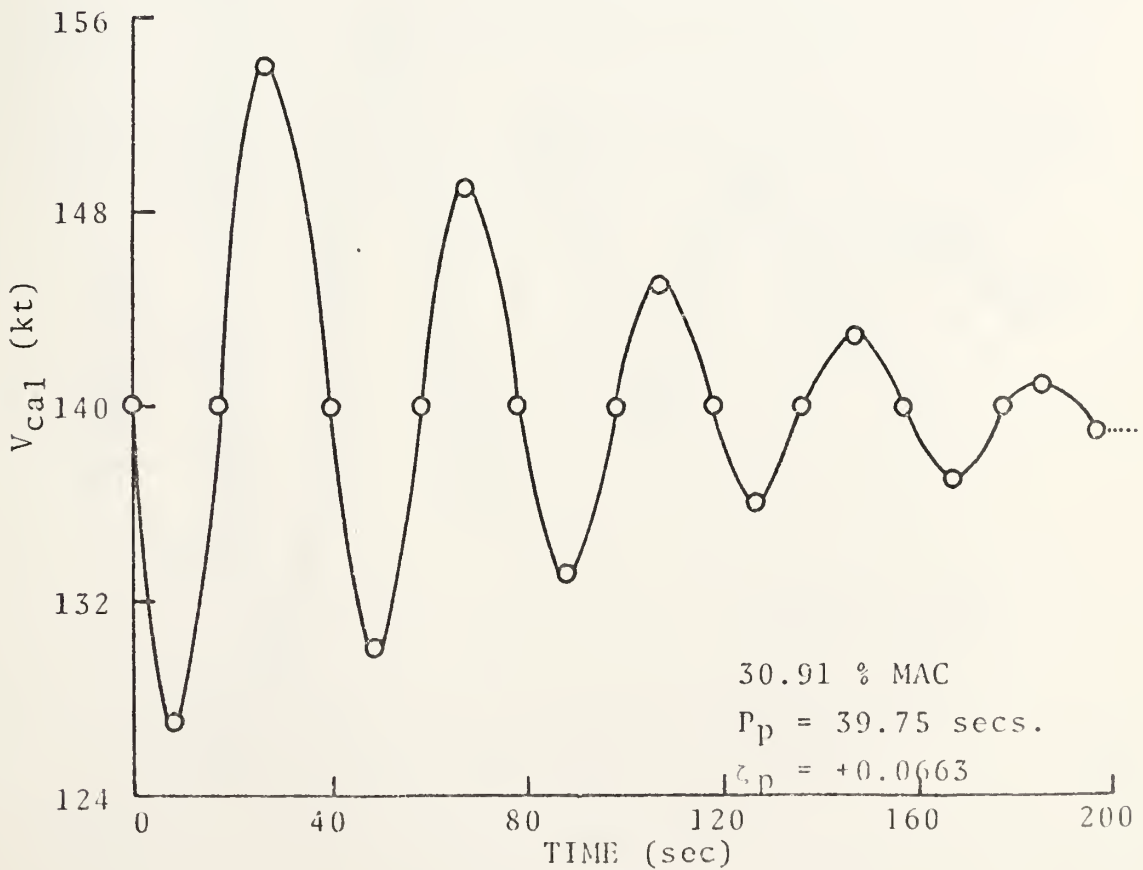
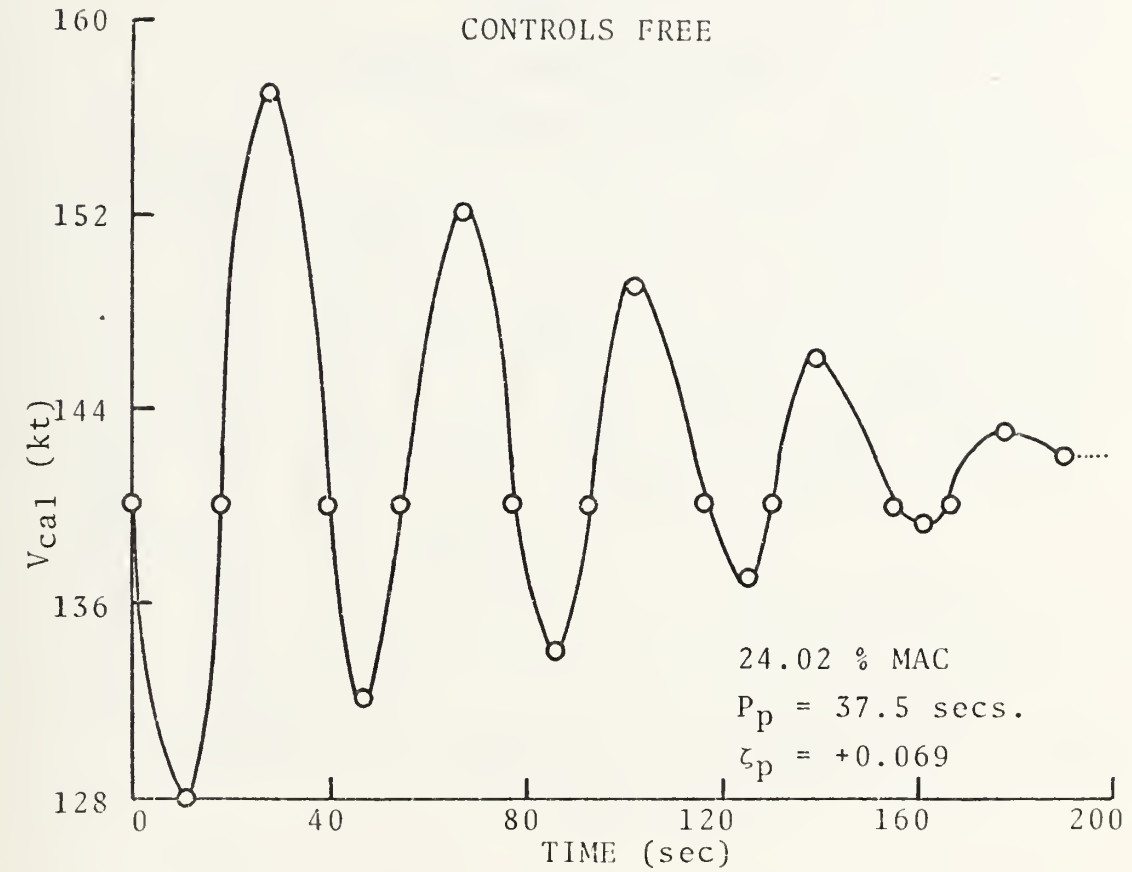
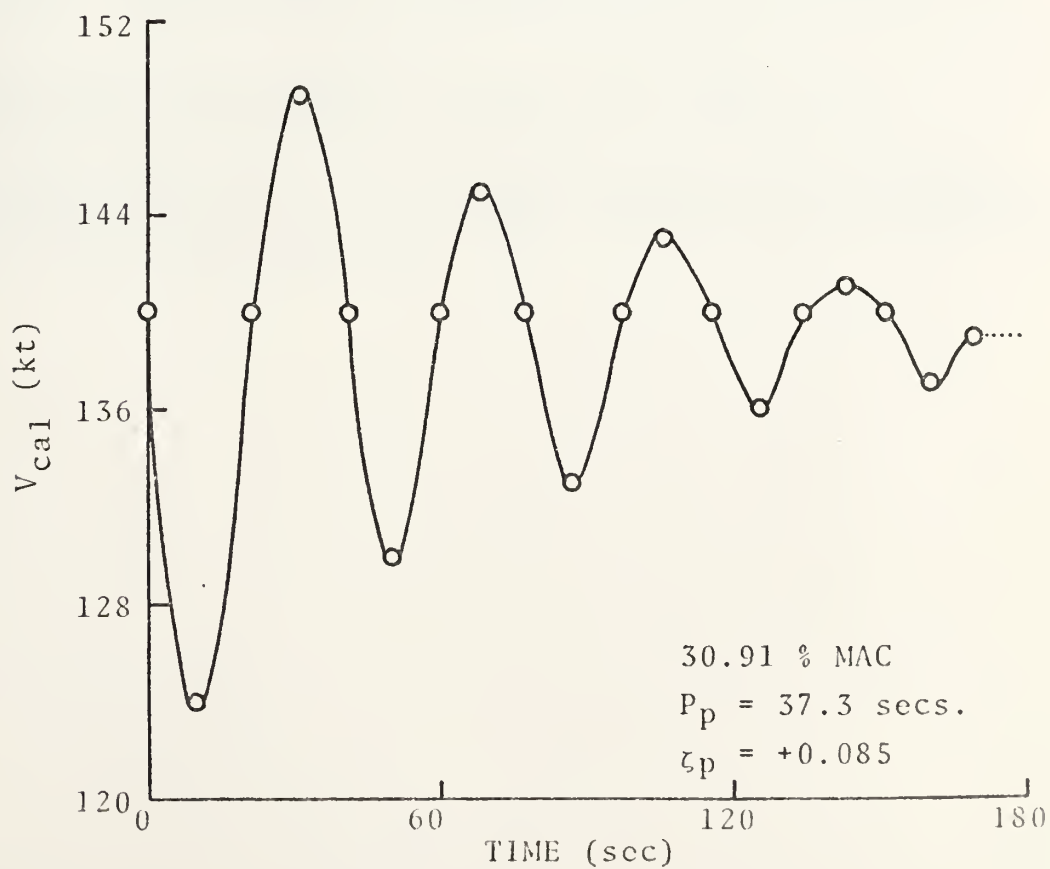
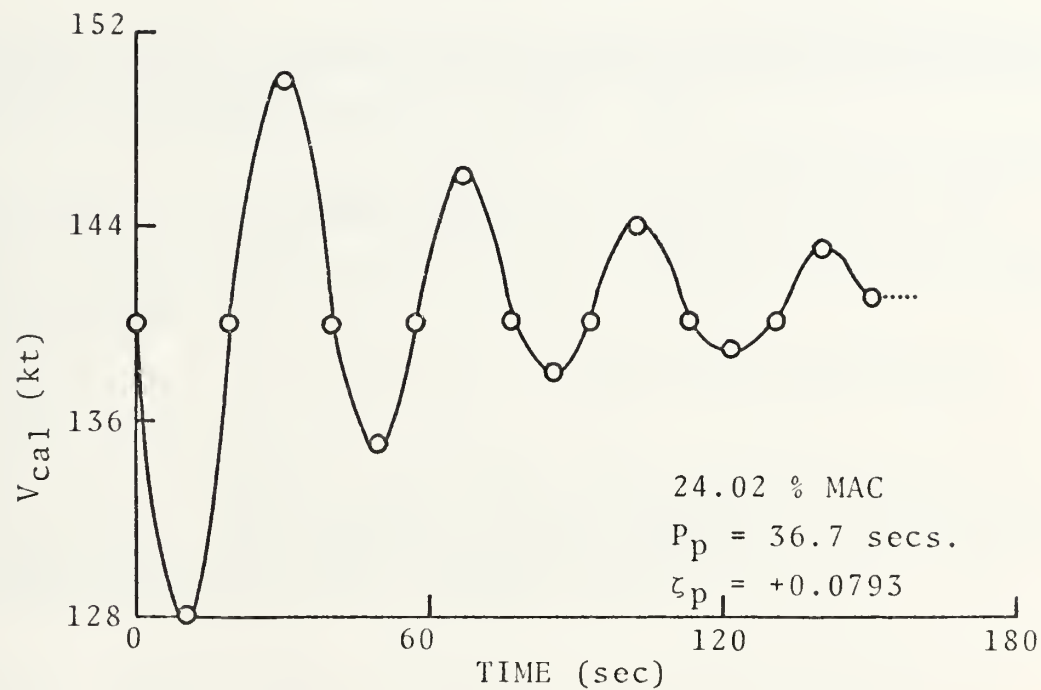


Figure 29

PHUGOID CHARACTERISTICS

CONTROLS FIXED



LIST OF REFERENCES

1. Advisory Group for Aeronautical Research and Development, Flight Test Manual, Vol. II, Stability and Control, edited by C. D. Perkins, Pergamon Press, 1959.
2. Irving, F. G., An Introduction to the Longitudinal Static Stability of Low-Speed Aircraft, Pergamon Press, 1966.
3. Fixed Wing Stability and Control, Theory and Flight Test Techniques, Naval Air Test Center, 1969.
4. Perkins, C. D. and Hage, R. E., Airplane Performance, Stability and Control, Wiley, 1949.
5. National Aeronautics and Space Administration Technical Note D-6238, A Wind-Tunnel Investigation of Static Longitudinal and Lateral Characteristics of a Full-Scale Mockup of a Light Twin-Engine Airplane, by M. P. Fink, J. P. Shivers, and C. C. Smith, Jr., April 1971.
6. Etkin, B., Dynamics of Flight, Stability and Control, Wiley, 1959.
7. Dommasch, D. O., Sherby, S. S., and Connally, T. F., Airplane Aerodynamics, 3d edition, Pitman, 1961.
8. United States Air Force Stability and Control Datcom, Project Engineer: D. E. Hoak, Principal Investigator: D. E. Ellison, McDonnell Douglas Corporation, October 1960, revised, September 1970.

INITIAL DISTRIBUTION LIST

	No. Copies
1. Defense Documentation Center Cameron Station Alexandria, Virginia 22314	2
2. Library, Code 0212 Naval Postgraduate School Monterey, California 93940	2
3. Department Chairman, Code 57 Department of Aeronautics Naval Postgraduate School Monterey, California 93940	2
4. Associate Professor D. M. Layton, Code 57-LN Department of Aeronautics Naval Postgraduate School Monterey, California 93940	1
5. LCDR William H. Siren, USNR 22698 Picador Drive Salinas, California 93901	1
6. Naval Air Systems Command Attn: AIR-320D Washington, D.C. 20360	1

Thesis

160732

S5395 Siren

c.1

A flight test
determination of the
static and dynamic
longitudinal stability
of the Cessna 310H
aircraft.

Thesis

160732

S5395 Siren

c.1

A flight test
determination of the
static and dynamic
longitudinal stability
of the Cessna 310H
aircraft.

thesS5395

A flight test determination of the stati



3 2768 002 01111 6

DUDLEY KNOX LIBRARY